Theory of Positron Annihilation in Solids*

RICHARD A. FERRELL

University of Maryland, College Park, Maryland

I. INTRODUCTION

IN the subject of annihilation of positrons in matter, the annihilation process itself can be considered to be well understood on the basis of quantum electrodynamics. The predictions of quantum electrodynamics in regard to the properties of positronium have been strikingly verified in dilute gases, where the positronium atom can be treated as an isolated two-body system with little interference from the other atoms of the gas. The experiment of Deutsch and co-workers, which established the radiative corrections in the fine structure splitting of the ground state of positronium, in particular, has confirmed with impressive accuracy the prediction of quantum electrodynamics. Such experiments have given one considerable confidence in the use of the annihilation process as a tool for the investigation of the interaction of positrons with matter under other circumstances. Surveys of the general subject of positron annihilation have been given by Deutsch[1] and by DeBenedetti and Corben.[2] Recently the application of positron annihilation as an experimental tool in solid state investigations has been considerably developed, and we confine ourselves to this topic.[2a] Here the annihilation process is used to investigate the low-energy electronic interactions which precede the annihilation.

One of the great virtues of the use of positrons as a tool is that a high-energy positron can penetrate into the interior of the sample and then be stopped and become a real member of the electronic system. This all happens very fast, and from then on one need only consider low-energy nonrelativistic interactions with the surrounding matter. As discussed in more detail later, the annihilation rate and the distribution in the total momentum of the annihilation photons emitted depend in many cases solely on the product of the positron wave function times the wave function of the electron being annihilated. Thus, experimental measurements of the lifetime and momentum distribution give useful information about the interior of the sample. An important advantage of the positron annihilation is that the information contained in the annihilation process is transported to the observer in high-energy gamma rays which escape without appreciable attenuation or scattering from reasonably small samples. This is in contrast to, say, the method of soft x-ray emission, where the surface properties of a solid under investigation may strongly influence the results. A drawback of the positron method is that, as is characteristic in atomic physics, the tool used for measuring the electronic structure itself changes the electronic structure. The positron distorts the electron wave functions, which must be corrected for in an interpretation of the experimental data. Most of the experimental data available so far have to do with the two-photon annihilation rate which is the predominant mode of decay in solids and liquids. Measurements of the three-photon rate have established that the slow two-photon decay which is observed in some insulators is associated with positronium production. The three-photon rate does not, however, give independent information since it is proportional to the product of the fraction of positrons which form positronium times the long lifetime, which was first discovered by Bell and Graham.[3] Both of these factors can be determined from the lifetime measurements alone. The three-photon annihilation experiments have been very valuable in clarifying the nature of the τ_2 component, and they will no doubt continue to be of great practical value as an independent determination of the parameters describing the two-photon annihilation. In this review, however, we limit the discussion to the two-photon mode of decay, since it in principle contains all the information so far obtained from the physical systems. In particular we discuss the two-photon lifetime and angular correlation.

Each individual interaction of an electron or positron with the radiation field can create only one photon. The annihilation process must proceed, therefore, by an intermediate state in which the original positron-electron pair is still present; in addition, one photon has been created. The photon has a momentum of the order of mc, where m is the mass of the electron and c the velocity of light. In the intermediate state, either the electron or the positron must be recoiling with approximately this same momentum. If the initial momentum of the particle is small compared to its change in momentum, as is the case with the slow electrons and positrons in which we shall be interested, the matrix element for the transition is to a good approximation independent of the initial momentum. The same holds for the transition from the intermediate to the final state, where the recoiling particle annihilates with the other member of the pair and emits the second photon. Therefore, the part of the second-order Hamil-

* Work supported by the Office of Naval Research.

[1] M. Deutsch, Progr. Nuclear Phys. 3, 131 (1953).

[2] S. DeBenedetti and Corben, Ann. Rev. Nuclear Sci. 4, 191 (1954).

[2a] See also the recent reviews by S. DeBenedetti, by R. E. Bell, and by M. Deutsch in *"Beta- and Gamma-Ray Spectroscopy,"* K. Siegbahn, Editor (North-Holland Publishing Company, Amsterdam, 1955), pp. 672, 680, and 689.

[3] R. E. Bell and R. L. Graham, Phys. Rev. **90**, 644 (1953).

tonian operator that produces a two-photon final state of total momentum $\hbar\mathbf{k}$ is proportional to

$$\sum_{\mathbf{k}_1}\sum_{\mathbf{k}_2} a_{\mathbf{k}_1} b_{\mathbf{k}_2} \delta_{\mathbf{k}_1+\mathbf{k}_2,\mathbf{k}}, \tag{i}$$

where $a_{\mathbf{k}_1}$ and $b_{\mathbf{k}_2}$ are plane wave annihilation operators for the electron and positron, respectively. The corresponding point annihilation operators $\varphi(\mathbf{x}_1)$ and $\psi(\mathbf{x}_2)$ can be introduced by means of the relations

$$a_{\mathbf{k}_1}=\frac{1}{\sqrt{V}}\int d^3\mathbf{x}_1 e^{-i\mathbf{k}_1\cdot\mathbf{x}_1}\varphi(\mathbf{x}_1),$$

$$b_{\mathbf{k}_2}=\frac{1}{\sqrt{V}}\int d^3\mathbf{x}_2 e^{-i\mathbf{k}_2\cdot\mathbf{x}_2}\psi(\mathbf{x}_2),$$

where V is the volume of quantization. Substituting into (i) and simplifying, one obtains

$$\int d^3\mathbf{x} e^{-i\mathbf{k}\cdot\mathbf{x}}\varphi(\mathbf{x})\psi(\mathbf{x}). \tag{ii}$$

Particularly simple special cases are (1) the system consists initially of only one electron-positron pair and (2) the initial wave function of a many-electron problem is a Slater determinant of orthonormal one-electron wave functions. In the first case the annihilation operators in (ii) simply become replaced by the Schrödinger wave function for the pair, evaluated for equal electron and positron coordinates. In the second case, application of (ii) to the Slater determinant yields as many terms as there are electrons. Each term is a Slater determinant of next lower degree and is multiplied by a numerical factor formally identical to (ii). In each of these factors the annihilators in (ii) are replaced by the "wave-function product," $\varphi(\mathbf{x})\psi(\mathbf{x})$, where now the functions signify electron and positron wave functions, evaluated at the same point. Thus, in case (2) the momentum distribution of the two-photon states arising from the annihilation of an electron-positron pair is obtained by squaring the absolute value of the Fourier transform of the "wave-function product."

The total annihilation rate is easily obtained by taking the matrix element of (ii) between the initial and final states, squaring the absolute value, and summing over all final states of the matter system as well as over all values of $\mathbf{k}$. The result is proportional to the expectation value, over the initial state, of the operator

$$\int d^3\mathbf{x}(\varphi^*(\mathbf{x})\varphi(\mathbf{x}))\cdot(\psi^*(\mathbf{x})\psi(\mathbf{x})). \tag{iii}$$

(iii) is simply the electron density operator at the position of the positron, averaged over the positron position. The proportionality constant can be established from the ground state of positronium which serves as a convenient reference case. There the electron density at the positron is $1/8\pi a_0^3$ while the spin-averaged annihilation rate as shown in the appendix, is 2.01×10^9 sec^{-1}.

II. IONIC CRYSTALS

A. Nonformation of Positronium

Positron annihilation studies have so far been carried out on a limited number of different ionic crystals. Bell and Graham[3] found that crystals of α-quartz and NaCl exhibit only prompt positron decay, with lifetimes of $(2.0\pm0.3)\times10^{-10}$ sec and $(2.3\pm0.3)\times10^{-10}$ sec, respectively. This behavior is in contrast to the almost universal presence in gases[1] and the widespread occurrence in insulating solids and liquids[3] of an additional relatively slow mode of decay. It is generally accepted that this slow mode of decay is due to the formation of positronium, which is probably best regarded as a natural and common fate of a positron being slowed down. If it is energetically possible for a positron passing through an insulator to capture an electron, it will generally do so, yielding a positronium atom more or less isolated and "protected" from the electrons bound in the surrounding atoms.[4] The situation in metals is much different, of course, and will be dealt with in the next section. In metals the conduction electrons are free to interfere with any positronium atom which might be formed, and can either strongly modify the positronium or prevent its independent existence altogether. In insulators, however, positronium formation seems to be a normal occurrence. The ionic crystals evidently comprise a special class in which the formation of a positronium atom, stable with respect to subsequent dissociation, is energetically not permitted.

The energetics of positronium formation in gases were first discussed by Ore[5] and have been reviewed by Deutsch.[1] Ore's analysis can be applied, with very little modification, to positronium formation in solids. In Fig. 1(a) is shown an "Ore diagram" for an ionic crystal, where for the moment the coulomb interaction energy between the positron and the ions is not taken into account. The left-hand portion shows the possible initial states of the system and is shaded below V_1, the bottom of the conduction band. Positronium formation by positrons of energy greater than V_1 can be ignored. A positronium atom thus formed will break up in subsequent collisions, resulting in a free positron of lower energy and a free electron—(the latter now in the conduction band).[6,7] The possible final states available to

[4] The formation of positronium in condensed materials has been discussed by P. R. Wallace [Phys. Rev. **100**, 738 (1955)].

[5] A. Ore, Univ. Bergen Årbok, No. 9 (1949).

[6] In the present analysis the excitation potential, V_1, plays a different role than that discussed in reference 1. There, in the case of gases, it represents a localized excited state which has the secondary role of competing with electron capture. It does not represent a state which can result from positronium break up,

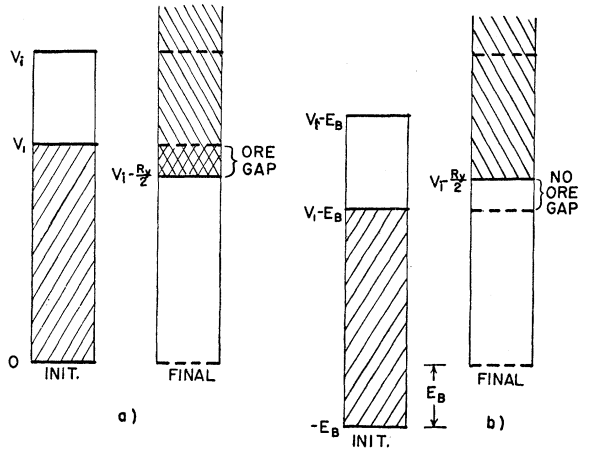

FIG. 1. The Ore diagram for (a) no energy shift (b) energy shift. The energy shift destroys the Ore gap and prevents positronium formation.

the system after the capture of an electron by a positron are shown by the shaded region of the right-hand portion of Fig. 1(a). Because of the requirement of energy conservation, the capture process can only take place if the two shaded regions overlap, forming the "Ore gap." The condition that there be an Ore gap is simply $V_1 > V_i - \text{ry}/2$, where ry/2 is the positronium binding energy of one-half rydberg, and V_i is the ionization potential (that is, the energy required to take an electron from the top of the valence band and remove it from the crystal).

Thus we see that the ionic crystals, where the bottom of the conduction band is below the ionization potential ($V_1 < V_i$), are on this account already somewhat unfavorable for positronium formation. This general feature is a result of the ordering of the ions in a regular lattice and disappears when sufficient disorder is introduced to destroy the conduction band. Then the Ore diagram should be drawn from V_i as the reference level. The ionic crystals are also quite different in this respect from the molecular crystals, where there is in general no electron energy band not already filled which is significantly below the ionization potential. This type of crystal is thus in the same category as the gases, where the Ore diagram is based on V_i as the reference level, ensuring positronium formation, or at least ensuring the existence of the Ore gap. In gases the other factors discussed below are also favorable.

In the ionic crystals there is an additional consideration based on the energetics which must be introduced into the Ore analysis, and which may also operate effectively against positronium formation. This is illustrated in Fig. 1(b) and has to do with the lowest non-positronium state of the positron in the system. Let E_B be the positron binding energy, i.e. the energy required to take a positron out of this state and remove it from the crystal. Then if positrons of energy greater than $V_1 - E_B$ capture electrons the resulting positronium atoms can break up again. The net result is to slow down the positrons by excitation of electrons into the conduction band. Thus this transitory formation of positronium can be ignored and the only lasting positronium formation comes from positron energies less than $V_1 - E_B$. The effect of binding of positronium to the crystal is not shown in Fig. 1(b) but must also be included. The criterion for the Ore gap must therefore be modified to read $V_1 - E_B > V_i - \text{ry}/2 - E_P$ or

$$(V_i - V_1) + E_B - E_P < \text{ry}/2, \tag{1}$$

where E_P is the binding energy of positronium atoms to the crystal. In analogy with general usage,[8] by which the quantity $V_i - V_1$ is called the "electron affinity," we shall call E_B and E_P the "positron affinity" and the "positronium affinity" of the crystal, respectively. The condition that there be positronium formation, or at least that there exist an Ore gap, is therefore simply that the sum of the electron and positron affinities minus the positronium affinity shall be less than the positron binding energy of 6.78 ev. Thus we see that the affinity of the crystal for positrons works equally as effectively as the affinity for electrons against positronium formation, while affinity of the crystal for positronium works in favor of positronium formation.

Before proceeding to discuss the affinities in more detail, it should be mentioned that there is in general an additional mechanism which operates against positronium formation. This is the depletion of the Ore gap by fast moderation of the positrons which happen to fall into it. Whenever there are excited states of the system below the reference level for the Ore diagram, the positrons can lose energy and leave the gap before capturing electrons.[6] This effect can be produced in the case of gases by introducing a relatively small concentration of a polyatomic gas. Since the latter has generally a large number of low-lying vibrational states, the positrons lose energy much more rapidly than otherwise. This results in a decrease, as has been observed by Dulit *et al.*,[9] in the percentage of positronium formation. In the case of the ionic crystals the positrons may be removed from the Ore gap by excitation of excitons, whose energies lie generally one or two electron volts below the conduction band,[10] and by excitation of phonons in the optical band. It is conceivable that in some cases this effect may so severely deplete the Ore gap that, although Inequality (1) may be satisfied, there is not enough positronium formation left to be

and is therefore not used as the reference level in drawing the Ore diagram.

[7] The breakup of the fast positronium atoms has been discussed by J. A. Wheeler, Ann. N. Y. Acad. Sci. 48, 219 (1946).

[8] N. F. Mott and R. W. Gurney, *Electronic Processes in Ionic Crystals* (Clarendon Press, Oxford, 1940), p. 73.

[9] Dulit, Gittelman, and Deutsch, Bull. Am. Phys. Soc. Ser. II, 1, 69 (1956).

[10] F. Seitz, *The Modern Theory of Solids* (McGraw-Hill Book Company, Inc., New York, 1940), Chap. XII.

detected experimentally. This does not seem likely, however, since requiring the depletion effect to predominate puts rather heavy demands on the slowing-down mechanism. The latter would have to complete with the relatively large electron-capture cross section.[11] For this reason we ignore the effect of depletion in the subsequent discussion.

To summarize the foregoing discussion, there are three basic factors which must be called upon to explain the absence of positronium formation in the ionic crystals:

(1) Electron affinity.
(2) Positron affinity.
(3) Positronium affinity.

These are, of course, general considerations, and can be used to understand the behavior of positrons in any insulating material.

The alkali halides are the simplest ionic crystals to treat theoretically, and we now proceed to try to estimate, for this special case, the relative importance of the three factors listed in the preceding paragraph. Beginning with (1), the electron affinity of the alkali halides can be established experimentally, independently of positron effects, and is of the order of an electron volt.[12–14] We therefore pass on to (2), and attempt a rough estimate of the positron affinity.

If one neglects the polarization of ions, he may assume that the positron in an ionic crystal moves under the influence of the Hartree-Fock self-consistent electrostatic field. The positron is repelled by the positive ions and attracted by the negative ions, unless it penetrates through the outer electron shells of the latter and experiences the strong repulsive Coulomb fields of the nuclei. Such a field for an isolated negative ion is shown schematically in Fig. 2, where the repulsive field of the nucleus is indicated by the dashed line. The minimum in the curve will occur, in a very crude approximation, at the Goldschmidt ion radius,[15–17] a, since the latter is also roughly equal to the radius of the outer portion of the electron cloud. The rapid rise in the potential for radii less than a can be approximated by an infinitely hard repulsive core. The potential is roughly a pure Coulomb field for radii greater than a. Although the true periodic potential in the crystal is, of course, not

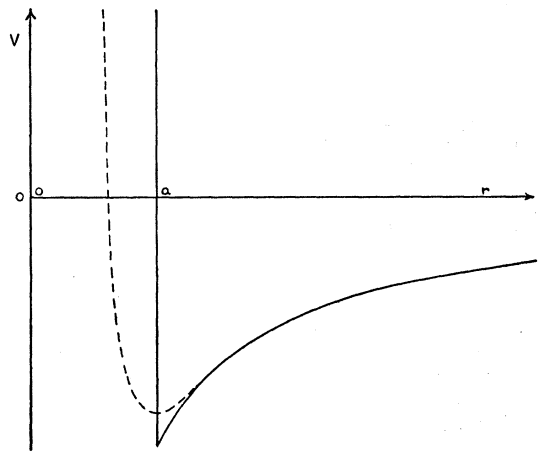

FIG. 2. Hard core idealization of the potential field around a negative ion. The dashed curve shows schematically the true potential.

that of an isolated ion, it will have in the immediate neighborhood of the negative ions the behavior shown in Fig. 2. Since the positron wave functions tend to be concentrated about the negative ions, one can expect a treatment on the basis of an isolated ion to give at least an order-of-magnitude estimate for the positron affinity. In other words, we treat the periodic potential problem by the tight binding approximation.[18]

It is a straightforward mathematical problem to solve the Schrödinger equation for the potential shown in Fig. 2, namely,

$$V(r)=\infty, \quad r<a \quad \text{and} \quad V(r)=-e^2/r, \quad r>a. \tag{2}$$

For an arbitrary value of the energy, the solution which is well-behaved as $r\to\infty$ is a confluent hypergeometric function. Imposing the additional boundary condition that the wave function vanish at $r=a$ determines the energy eigenvalue. Such a procedure has been followed by Jastrow[19] in a somewhat similar problem, but is mathematically more involved than the accuracy of the present considerations warrants. Instead we satisfy ourselves here with an estimate of the ground state binding energy based on the Rayleigh-Ritz-Schrödinger variational principle.[20]

As trial function we choose $\psi(r)=(4\pi)^{-\frac{1}{2}}\chi(r)/r$, where for $r\geq a$,

$$\chi(r)=C(r-a)e^{-(r-a)/b}. \tag{3}$$

The normalization constant, C, in terms of the variational parameter, b, is given by $C=2b^{-\frac{3}{2}}$. Introducing the dimensionless parameter $\gamma=2a/b$, we find the ex-

[11] The calculations of H. S. W. Massey and C. B. O. Mohr [Proc. Phys. Soc. (London) **A67**, 695 (1954)] show that the capture cross section in a gas is of the order of atomic dimensions. See also C. B. O. Mohr, Proc. Phys. Soc. (London) **A68**, 342 (1955).

[12] See reference 8, pp. 73, 97.

[13] L. Apker and E. Taft, *Imperfections in Nearly Perfect Crystals* (John Wiley and Sons, Inc., New York, 1952), p. 246.

[14] F. Seitz, Revs. Modern Phys. **26**, 7 (1954). See in particular, pp. 83–87.

[15] V. M. Goldschmidt, Skrifter Norskl Videnskaps- Akad. Oslo I. Mat. Naturv. Kl. **1926**.

[16] Landolt-Bornstein, *Zahlenwerte und Funktionen* (1955), Vol. I, Part 4, pp. 523–527.

[17] G. Leibfried, *Handbuch der Physik* (Springer-Verlag, Berlin, 1955), Vol. VII, Part 1, pp. 132–143.

[18] Views similar to those of this paragraph have been expressed by DeBenedetti, Cowan, Konneker, and Primakoff, Phys. Rev. **77**, 205 (1950).

[19] R. Jastrow, Phys. Rev. **73**, 60 (1948). See also A. Sommerfeld and H. Welker, Ann. Physik **32**, 56 (1938).

[20] L. Schiff, *Quantum Mechanics* (McGraw-Hill Book Company, Inc., New York, 1955), second edition, pp. 171–172.

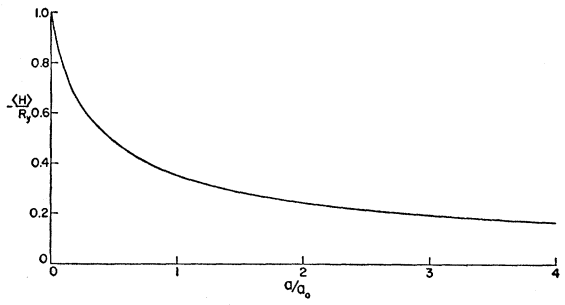

FIG. 3. Estimate of the energy of binding (in Rydbergs) of a positron to a negative ion as a function of the hard core radius (in Bohr radii).

pectation value of the kinetic energy to be

$$\langle T\rangle=\frac{\hbar^2}{2m}\int_a^\infty\left(\frac{d\chi}{dr}\right)^2 dr=\tfrac{1}{4}\ \mathrm{ry}\left(\frac{a_0}{a}\right)^2\gamma^2. \tag{4}$$

The expectation value of the potential energy is

$$\langle V\rangle=-e^2\int_a^\infty \chi^2\frac{dr}{r}$$
$$=-\mathrm{ry}\left(\frac{a_0}{a}\right)[\gamma-\gamma^2-\gamma^3e^\gamma\ \mathrm{Ei}(-\gamma)]. \tag{5}$$

The function

$$\mathrm{Ei}(-\gamma)=-\int_\gamma^\infty e^{-x}\frac{dx}{x}$$

is tabulated by Jahnke and Emde.[21] Requiring the expectation value of the total energy, $\langle H\rangle=\langle T\rangle+\langle V\rangle$, to be a minimum yields, after differentiating Eqs. (4) and (5) and setting the sum to zero, the relation

$$\frac{a}{a_0}=\frac{\gamma}{2f(\gamma)}, \tag{6}$$

where

$$f(\gamma)=1-2\gamma-\gamma^2-(3\gamma^2+\gamma^3)e^\gamma\ \mathrm{Ei}(-\gamma).$$

This gives for a lower bound of the binding energy, measured in rydbergs, the value

$$-\frac{\langle H\rangle}{\mathrm{ry}}=f(\gamma)\cdot g(\gamma), \tag{7}$$

where

$$g(\gamma)=1+\gamma^2+(\gamma^2+\gamma^3)e^\gamma\ \mathrm{Ei}(-\gamma).$$

The right-hand side of Eq. (7) can be computed for various values of γ. The core radii which correspond to these energies can then be found from Eq. (6). The result of such a computation is shown in Fig. 3. For small values of a/a_0 the quantity $-\langle H\rangle/\mathrm{ry}$ drops rapidly, according to $1-4(a/a_0)$. The plot of $-\langle H\rangle/\mathrm{ry}$ *vs* a/a_0 then levels off for larger values of a/a_0 and in the region $2\leq a/a_0\leq 4$ gives a positron binding energy which varies from 0.24 rydberg to 0.17 rydberg. The accuracy of this approximate solution to the mathematical problem posed by the idealized potential function of Eq. (2) can be established by considering the $2s$ wave function of the hydrogen atom. This function has a radial node at $r=2a_0$, and for $r\geq 2a_0$ provides an exact solution to our problem in the case $a=2a_0$. The corresponding exact value for the binding energy is 0.25 rydberg, in good agreement with the above approximate value.[22]

A check on our hard core idealization of the positron binding problem in the case of the chloride ion is provided by Simons'[23] exact calculation based on the Hartree-Fock self-consistent field.[24] Simons finds a binding energy of the positron in the ground state of 3.74 ev. From the Cl^- radius of 1.81 A, (see reference 16, and Table I later), we have $a/a_0=3.42$, which gives, according to Fig. 3, $-\langle H\rangle=0.175$ ry $=2.37$ ev. Thus we see that our procedure considerably underestimates the true binding energy of a positron to a negative ion. This is attributable mainly to incorrect choice of hard core radius. As seen from Fig. 2, a more realistic choice of effective core radius would be considerably smaller than the Goldschmidt radius. Allowing for this we can conclude that the binding energy of a positron to an isolated halide ion amounts to 3–5 ev.

The above positron binding energy estimate for an isolated halide ion can be applied to the positron binding to an alkali halide crystal, providing the effect of the neighboring ions is taken into account. If it is assumed that the effect on the positron wave function can be neglected, the only effect of the surrounding ions is to raise the energy by the Madelung term.[25] If c is one-half the interatomic spacing this amounts to 1.74 ry(a_0/c) for a simple cubic crystal, and is of the same order as the binding to an isolated halide ions. The estimate obtained in the previous paragraph is therefore severely reduced, and it becomes questionable whether there remains even a net positive positron affinity.† In any case we can conclude that the sum of the electron and positron affinities is of the order of 1–2 ev and falls far short of accounting for the absence of an Ore gap.

It remains only to discuss (3), the positronium affinity of the alkali halides. This is difficult to estimate ac-

[21] E. Jahnke and F. Emde, *Tables of Functions* (Dover Publications, New York, 1945), pp. 1–9.

[22] The other *ns* wave functions of the hydrogen atom provide additional checks. The next most tightly bound solution, however, has its outermost radial node at $7.2a_0$, which corresponds to a hard core radius outside the present range of interest.

[23] L. Simons, Phys. Rev. **90**, 165(L) (1953).

[24] D. R. Hartree and W. Hartree, Proc. Roy. Soc. (London) **A156**, 45 (1936).

[25] See reference 8, p. 71.

† *Note added in proof.*—The experiment of Madansky and Rasetti [L. Madansky and F. Rasetti, Phys. Rev. **79**, 397 (1950)], provides a method of experimentally settling this question. They find that positrons do not diffuse through and leave thin films of glass, mica, celluloid, and octoil. There must, therefore, be a net positive positron affinity in these substances.

curately, but simple considerations suffice to show that it is probably very large, and negative. If a positronium atom is to be brought into such a crystal it must be introduced interstitially. But the interstitial space available is extremely limited, since it is only that left between packed spheres of 1–2 A radius. Thus, the positronium atom is confined to a space of dimensions at most of the order of 1 A. This greatly lowers its internal binding energy (see reference 18), thereby contributing, in the extreme case that there is no bound state remaining, $-\text{ry}/2$ to the positronium affinity. An additional contribution comes from the zero point motion of the positronium atom. Even if it has enough room to retain its identity as a bound system, the confinement of one of its center-of-mass degrees of freedom to a "free run" of, say, $2a_0$, or about 1 A, results in additional kinetic energy of the atom of $(\pi^2/8)\ \text{ry}=16.7$ ev. This effect is peculiar to the positronium atom and is due to its anamalously small mass.

Thus we see that there are two sources of very large negative positronium affinity, more than adequate to violate Inequality (1) and destroy the Ore gap. This is doubtless a general feature of all the ionic crystals and is essentially simply due to the fact that there is no room in the crystals for a positronium atom.[26] Such a reason could have of course, been proposed at the very start of this section, but it was thought desirable to discuss the problem from the general standpoint of the energetics of the electron capture process. The discussion will also be useful as background for the next section and for Sec. IV, where the solids in which positronium is formed are studied.

B. Two-Photon Angular Correlation

As discussed in the preceding section, positrons which enter an ionic crystal do not capture electrons because there is no room in the crystal for the resulting positronium atoms. Better, the limited space available to positronium atoms leads to a large negative positronium affinity, and consequently no Ore gap. In any case, the positrons remain, during the slowing down process, in nonpositronium states, and it seems likely that they will become thermally moderated in a time short compared to the annihilation lifetime of the order of 10^{-10} sec. This is because of the strong coupling of a charged particle to the optical band phonons, and may not be true in non-ionic crystals (see reference 4). The small thermal energy may be neglected for the present purposes, and the annihilation considered as taking place from the ground state of the system of positron plus crystal.

The lifetimes found experimentally are of the order of magnitude of what can be expected on the basis of the type of ground-state wave function discussed in the preceding section. There it was shown that the positron wave function is concentrated about the negative ions into a bound s wave, with a maximum at about the ion radius, a. The electrons on the other hand, can be roughly thought of as uniformly spread out over the volume of a sphere of radius a. Only the eight electrons occupying the noble gas configuration come into question. (The more tightly bound electrons are in a region of high electrostatic potential and are consequently never "sampled" by the positron.) Consequently the ratio of the electron density at the positron in terms of that in the positronium atom, which provides a convenient density unit for comparison, is

$$\frac{8}{(4\pi/3)a^3}\Big/\frac{1}{8\pi a_0^3}=48\left(\frac{a_0}{a}\right)^3.$$

As stated in the preceding section, for the chloride ion $a/a_0=3.42$, giving for the above density ratio the value 1.20. Since the positron lifetime is inversely proportional to the electron density, we divide the spin-averaged positronium lifetime by this density ratio and obtain 4.16×10^{-10} sec for the lifetime of a positron bound to a chloride ion. Since six of the eight electrons in the noble gas configuration have p symmetry and vanishing density at the ion nucleus, the uniform distribution used above should probably be replaced by a nonuniform distribution concentrated at a radius somewhat smaller than the ion radius. Therefore the electron density at the positron is probably larger than the estimate given above. Thus it is likely that a more exact calculation may give a lifetime only half as large as our rough estimate, and thereby in agreement with the experimental value[3] of $(2.3\pm0.3)\times10^{-10}$ sec. Although the present crude approach does not yield reliable absolute values for the lifetimes it does predict a dependence on the ion radius which it would be interesting to check with further experiments on the alkali halides. The lifetime should depend only on the halide ion and should be proportional to the cube of the ion radius. This quantity varies by a factor of 4.5 in going from F^- to I^-. We should therefore expect F^- and I^- to exhibit significantly shorter and significantly longer positron lifetimes, respectively, than Cl^-. There may be some polarization of the electron shell by the positron which may also somewhat reduce the lifetime below the above rough estimate, but this effect is evidently not large in the case of NaCl. Thus there does not seem to be any difficulty in understanding the lifetimes. We therefore proceed to interpret the recent experimental results of Lang and DeBenedetti[27,28] on the angular correlation of the two photons given off by the annihilation of positrons in crystals of the alkali halides.

As explained in the Introduction, the probability

[26] The need for room in order to have positronium formed in a solid has been emphasized by V. L. Telegdi [Bull. Am. Phys. Soc. Ser. II, 1, 168 (1956)].

[27] G. Lang and S. DeBenedetti, Bull. Am. Phys. Soc. Ser. II, 1, 69 (1956).

[28] S. DeBenedetti, Bull. Am. Phys. Soc. Ser. II, 1, 115 (1956).

that the two annihilation photons carry off a certain amount of total momentum is proportional to the absolute square of the corresponding Fourier transform of the "wave-function product." The latter is the product of the wave functions of the annihilating positron and electron. Since we are dealing with crystals we must consider that the wave functions, even in the tight binding approximation, are Bloch waves spread out over the entire crystal lattice. The positron is in the state of lowest crystal momentum, and therefore its wave function at any point in the crystal is simply equal to $1/\sqrt{N}$ times the wave function representing the positron bound to the nearest halide ion. The normalization constant depends on N, the number of halide ions in the crystal. On the other hand, the electrons with which the positron can annihilate possess values of the crystal momentum which fill up the first Brillouin zone. The wave function for an electron of crystal momentum $\hbar\mathbf{K}$ is equal at any point to the wave function representing the electron bound to the nearest halide ion times $(1/\sqrt{N})e^{i\mathbf{K}\cdot\mathbf{x}_n}$, where $\mathbf{x}_n$ is the position vector of the halide ion. The Fourier transform corresponding to momentum $\hbar\mathbf{k}$ is therefore the factor

$$F_{\mathbf{K}}(\mathbf{k})=\frac{1}{N}\sum_n e^{-i(\mathbf{k}-\mathbf{K})\cdot\mathbf{x}_n}$$

times the Fourier transform for annihilation by an isolated ion, where the sum extends over all halide ions. The sum is negligibly small except when $\mathbf{K}$ is equal to, or nearby equal to, $\mathbf{k}$ plus some multiple of the reciprocal lattice vector. The total annihilation probability is the absolute square of the Fourier transform for annihilation by an isolated ion times

$$\sum_{\mathbf{K}}|F_{\mathbf{K}}(\mathbf{k})|^2=\frac{1}{N^2}\sum_n\sum_m e^{i\mathbf{k}\cdot(\mathbf{x}_n-\mathbf{x}_m)}\sum_{\mathbf{K}}e^{-i\mathbf{K}\cdot(\mathbf{x}_n-\mathbf{x}_m)}.$$

The $\mathbf{K}$ sum is over the entire Brillouin zone. Since $\mathbf{x}_n-\mathbf{x}_m$ is a lattice vector the sum vanishes unless $n=m$. Therefore

$$\sum_{\mathbf{K}}|F_{\mathbf{K}}(\mathbf{k})|^2=1,$$

and the annihilation properties of a crystal are the same as those of the constituent isolated ions, provided the tight binding approximation applies.

Returning now to the wave-function product for an isolated halide ion, we can replace in a very rough approximation the positron wave function by

$$\psi(r)=\frac{1}{(4\pi)^{\frac{1}{2}}}\delta(r-a). \tag{8}$$

This possesses the spherical symmetry of the true wave function, but exaggerates the peaking of it at the ion radius to such an extent that $\psi(r)$ is no longer normalizable. This will, however, only affect the high momentum components of the Fourier transform and can be taken into account later. Actually, the positron wave function enters the analysis only through its product with the electron radial wave function. Because of the rapid fall off in the latter for $r>a$, and the fall off in the positron wave function for $r<a$, the product will be rather sharply peaked even if the positron wave function is not. Thus, Eq. (8) is not necessary for the following work but is introduced for convenience. The final results are largely independent of it.

The Fourier transform can easily be evaluated by introducing spherical polar coordinates with polar axis along the momentum $\hbar\mathbf{k}$, and making the well-known expansion of the momentum factor[29]:

$$e^{-i\mathbf{k}\cdot\mathbf{x}}=\sum_{l=0}^{\infty}(2l+1)(-i)^l j_l(kr)P_l(\cos\theta). \tag{9}$$

θ is the angle between the polar axis and the position vector $\mathbf{x}$, P_l are the Lengendre polynomials, and j_l the spherical Bessel's functions.[30] Let us first consider the annihilation of an s electron, of wave function

$$\phi_s(r)=\frac{1}{(4\pi)^{\frac{1}{2}}}R_s(r).$$

Then, substituting from Eqs. (8) and (9), the Fourier transform reduces to

$$\int e^{-i\mathbf{k}\cdot\mathbf{x}}\phi_s\psi d^3\mathbf{x}=a^2R_s(a)j_0(ka), \tag{10}$$

where all terms of the infinite sum have dropped out except the one for $l=0$. The probability that the positron and s electron will annihilate and yield two gamma rays carrying away a total momentum of $\hbar\mathbf{k}$ is therefore proportional to $a^4R_s(a)^2j_0(ka)^2$. It is convenient for purposes of subsequent integration to approximate the k-dependent factor by a simple Gaussian adjusted to give the right fall off at $k=0$. As shown in Fig. 4 where the approximate curve (H_s) is compared to the exact curve (G_s), this procedure fails to reproduce the weak secondary maxima of the spherical Bessel's function. These, however, arise from the approximation made in Eq. (8), and as explained there, should be neglected anyway. Therefore, dropping the factor a^4, the relative probability of s annihilation is approximately

$$P_s(k)=R_s(a)^2e^{-(ka)^2/3}. \tag{11}$$

The annihilation with the p electrons can be handled similarly. With the above choice of coordinates, only the $m=0$ state can annihilate and yield two photons whose total momentum is in the direction of the polar axis. Writing the wave function for such a state as $\phi_p=(3/4\pi)^{\frac{1}{2}}R_p(r)P_1(\cos\theta)$, and noting that now only

[29] See reference 20, p. 104.
[30] See reference 20, p. 77.

the $l=1$ term in the series expansion contributes, we obtain

$$\int e^{-i\mathbf{k}\cdot\mathbf{x}}\phi_p\psi d^3\mathbf{x}=-i\sqrt{3}a^2R_p(a)j_1(ka). \quad (12)$$

Here we make the approximation

$$\left(3\frac{j_1(\rho)}{\rho}\right)^2\equiv G_p(\rho)=\left(3\frac{\sin\rho-\rho\cos\rho}{\rho^3}\right)^2$$
$$\approx e^{-\rho^2/5}\equiv H_p(\rho). \quad (13)$$

This approximation is illustrated in Fig. 5, where the abscissa is $\rho=ka$, as is also the case in Fig. 4. Defining the relative probability for p annihilation as a^{-4} times the absolute square of Eq. (12), we have, approximately,

$$P_p(k)=\tfrac{1}{3}R_p(a)^2(ka)^2e^{-(ka)^2/5}. \quad (14)$$

Experimentally it is not possible to measure directly the probability distribution with respect to k, but only the distribution with respect to one of the Cartesian components of $\mathbf{k}$. Therefore it is necessary to calculate the integrals $\int\int P_{s,p}((k_x^2+k_y^2+k_z^2)^{\frac{1}{2}})dk_xdk_y$ in order to be able to make a comparison of theory with experiment. In the present problem it is convenient to introduce the variables

$$\zeta=k_za/\sqrt{5} \quad \text{and} \quad u=(k_x^2+k_y^2)a^2/5.$$

Then the probability distribution function for k_z is proportional to the function

$$P(\zeta)=\frac{3}{5R_p(a)^2}\int_0^\infty\left[P_p\left(\left(\frac{5}{a^2}(\zeta^2+u)\right)^{\frac{1}{2}}\right)+P_s\left(\left(\frac{5}{a^2}(\zeta^2+u)\right)^{\frac{1}{2}}\right)\right]du$$
$$=\exp(-\zeta^2)\int_0^\infty(\zeta^2+u)e^{-u}du+\frac{3}{5}\left(\frac{R_s(a)}{R_p(a)}\right)^2\times\exp(-5\zeta^2/3)\int_0^\infty\exp(-5u/3)du$$
$$=(1+\zeta^2)\exp(-\zeta^2)+C\exp(-5\zeta^2/3), \quad (15)$$

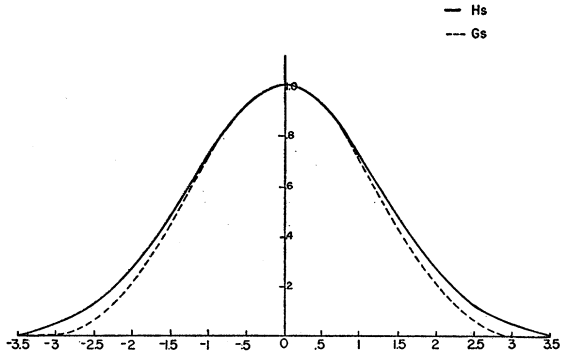

FIG. 4. Comparison of approximate function (solid curve) with exact function (dashed curve) for s electron annihilation.

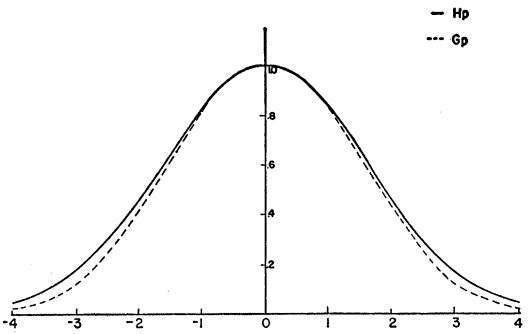

FIG. 5. Comparison of approximate function (solid curve) with exact function (dashed curve) for p electron annihilation.

where $C=(3R_s(a)/5R_p(a))^2$. Although the precise value of this constant depends on the particular halide ion under consideration, it can be expected to be of order of magnitude of, but somewhat smaller than unity. Figure 6 shows a plot of $P(\zeta)$ *vs* ζ for the arbitrary choice $C=0.6$. The individual contributions of s and p annihilation are shown by the dashed curves. The general feature of the composite curve, which holds over a fair range of values of C, is that the s contribution produces a fall off in $P(\zeta)$ at small ζ, where the p contribution is practically constant. The p contribution then falls off at larger ζ, yielding a triangular-shaped composite curve which has roughly constant slope over a wide range of ζ. Such a two-photon angular correlation has been reported as a general feature of the alkali halides by Lang and DeBenedetti.[27,28] They found that the several alkali halides investigated all have approximately this triangular distribution. They found further that the "cut-off angle," or the intercept of the linear portion of the curve, extended down to the horizontal axis, is a property primarily of the halide ion and is largely independent of the alkali ion with which it happens to be compounded. Such an extrapolation is shown in Fig. 6 and yields an intercept of $\zeta=1.80$. Introducing $\theta=\hbar k_z/mc$, the projected angle between the two annihilation photons, we find for the cut-off angle

$$\theta_c=1.80\times(5)^{\frac{1}{2}}\hbar/mca=(15.53/a) \quad (16)$$

milliradians, where a is now measured in angstrom units. Goldschmidt's values for the ion radii[16] give the predicted cut-off values appearing in Table I under the column "Theory." The values reported by Lang and

TABLE I. Two-photon angular correlation cutoff for the alkali halides.

Halide ion	Goldschmidt Ion radius a (in A)	Cutoff angle (in 10^{-3} radian) Theory $15.53/a$	Exp. (Lang and DeBenedetti)
F^-	1.33	11.68	10.6 (LiF)
Cl^-	1.81	8.58	8.0 (NaCl) 7.5 (KCl)
Br^-	1.96	7.92	...
I^-	2.20	7.06	6.7 (KI)

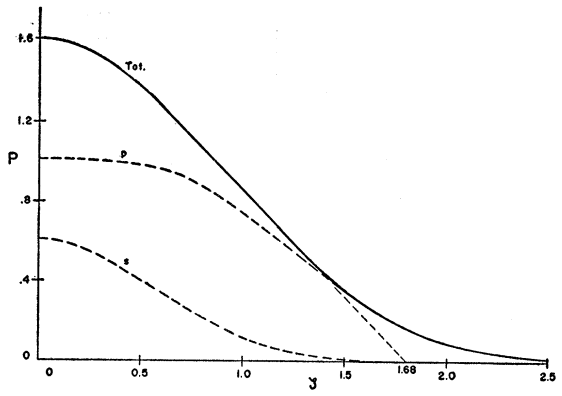

FIG. 6. Halide ion two-photon angular correlation as a function of $\zeta=(amc/\sqrt{5}\hbar)\cdot\theta$, where θ is the projected angle between the directions of the annihilation photons and a is the ion radius. 1.68 should be replaced by 1.80.

DeBenedetti are listed in the next column, and it will be noted that the agreement with the present crude theory is as good as could be expected. The basic limitation in the accuracy of the present approach, which neglects the influence of neighboring ions, is indicated by the experimental difference between the NaCl and the KCl cut-off angles, which amounts to 0.5 milliradian, or about 6%.

Equation (16) is obviously dependent, although not strongly, on the constant C. We have arbitrarily taken the value to be 0.6 for all the halides. This value does give the triangular-type distribution with about the longest linear portion. The fact that such a long linear portion is observed by Lang and DeBenedetti indicates that the above arbitrarily chosen value may be fairly close to the range of the true values. The latter could be determined by more detailed Hartree-Fock self-consistent field calculations. It is hoped that the present very rough work may indicate the direction in which refinements can be made and that it may serve to encourage more elaborate calculations.

III. METALS

A. Two-Photon Angular Correlation

As discussed in the preceding section, the probability of observing a certain angle between the two photons emitted by a positron and electron annihilating in a solid depends on the Fourier transform of the wave function product. Information can therefore be obtained on the electron wave function provided the positron wave function can be independently determined. Fortunately, this is the case, for the annihilation process is sufficiently slow to allow the positron to fall essentially into its ground state before the annihilation takes place. The ground-state wave function has particularly simple properties and can, in principle, be calculated to any desired accuracy. Although DeBenedetti *et al.*[18] have found that the time required for thermalization of positrons by a metallic lattice is of the order of the annihilation lifetime, the work of Garwin[30a] and the recent calculations of Lee-Whiting[31] make it clear that the slowing of the positrons by the conduction electrons is a much more important effect, leading to a net thermalization time very much shorter than the lifetime. Because of the smallness of the thermal energy, (at least at room temperature), compared to a characteristic electronic energy of the system, such as the Fermi energy, the positron can be considered as in its lowest energy state of zero crystal momentum. The wave function for this state is excluded from the volume occupied by the positive ions in the metal and has a sort of "Swiss cheese"[32] structure, being appreciably different from zero only in the interstitial regions. In regard to the electron wave functions, the modulation effects of the lattice on the Bloch waves are generally greatest in the region of the ions, where the positron wave function vanishes. Hence it is a reasonable first approximation, in considering the annihilation with the conduction electrons, to replace the Bloch waves which appear in the wave function products by unmodulated plane waves, with of course, the same crystal momenta.[33] A further simplification is suggested by the fact that in many metals the ions occupy a relatively small fraction of the total volume. It is therefore a useful additional approximation to neglect the "Swiss cheese" nature of the positron wave function altogether. Experimental evidence on the validity of these approximations will be discussed below.

When the above approximations have been made the problem has been reduced to that of the annihilation of a positron in a degenerate electron gas. With such an idealization, various metals can differ from one another only by virtue of different values of the density of conduction electrons. The electron density n thus plays a key role in the theory of positron annihilation in metals, (and, indeed, in the theory of metals in general). It is desirable to specify it in terms of the dimensionless parameter r_s, which measures the radius of the so-called unit electron sphere, in units of the Bohr radius.[34] By definition, the volume of the unit sphere, $4\pi a_0^3 r_s^3/3$, is equal to the volume per electron, $1/n$. If one uses the relation $n=(Lz\rho/A)$ cm^{-3}, where L is Avogadro's number, and z, ρ, and A the valence, specific gravity, and atomic weight of the metal, respectively, it is a simple matter to solve for r_s and reduce the resulting expression to the following formula involving only dimensionless quantities:

$$r_s=1.384(A/\rho z)^{\frac{1}{3}}. \tag{17}$$

[30a] R. L. Garwin, Phys. Rev. **91**, 1571 (1953).
[31] G. E. Lee-Whiting, Phys. Rev. **97**, 1557 (1955).
[32] This general picture has been given in the paper by DeBenedetti, Cowan, Konneker, and Primakoff (see reference 18), and has been given this graphic description by S. DeBenedetti (reference 28).
[33] This approximation is suggested by remarks made in the paper of Lang, DeBenedetti, and Smoluchowski [Phys. Rev. **99**, 596(L) (1955)].
[34] See reference 10, p. 340. We follow D. Pines (reference 55 later) in defining r_s so as to be dimensionless.

The Fermi momentum, $\hbar k_0$, or maximum momentum of an electron in the Fermi sea, is conveniently expressed in terms of the parameter r_s. From $n=k_0^3/3\pi$, one easily obtains

$$k_0=1.917/a_0r_s. \tag{18}$$

The two-photon angular correlation resulting from annihilation of a positron in an electron gas is particularly simple. The probability that a momentum $\hbar\mathbf{k}$ is conveyed to the photons is proportional to the absolute square of the Fourier transform of the wave-function product. But the latter vanishes except for the pair of electrons with exactly the momentum $\hbar\mathbf{k}$, in which case it is a constant independent of $\mathbf{k}$. (For a discussion of positron-electron correlation effects, which introduce a velocity dependence into the annihilation rate, see Sec. C later.) The probability distribution function is therefore proportional to the function $P(k)$, which vanishes for $k>k_0$ and equals the constant $1/\pi k_0^2$ for $k\leq k_0$. The distribution function for the z component of momentum is consequently

$$P_z(k_z)=\int\int P((k_x^2+k_y^2+k_z)^{\frac{1}{2}})dk_xdk_y=1-(k_z/k_0)^2. \tag{19}$$

This function represents an inverted parabola when plotted against k_z dropping to zero at the Fermi momentum. Equation (19) does not apply for $k_z>k_0$, in which case $P_z(k_z)=0$. The angle θ between the two planes defined by the two detector slits and the source is linearly related to k_z by $\theta=\hbar k_z/mc$. Hence the plot of the number of counts *vs* θ is also a parabolic function, proportional to $1-(\theta/\theta_0)^2$, where the cutoff occurs at the maximum angle (measured in milliradians) of

$$\theta_0=13.99/r_s. \tag{20}$$

The first experimental attempt to establish the connection between the two-photon angular correlation and the Fermi momentum was carried out by DeBenedetti *et al.*[18] They worked with the nonideal case of gold, in which the excluded volume effect is not negligible and tends to confuse the simple parabolic distribution. Green and Stewart,[35] working with the more ideal cases of the light elements, succeeding in establishing accurately the relation expressed by Eq. (20) between the breadth of the angular distributions and the Fermi momenta. These authors express their results in terms of an effective Fermi energy, which they find agrees in every case with the Sommerfeld value for the Fermi energy. It seems however, desirable to avoid interpreting this type of experiment, which depends only upon the electron momenta, in terms of electron energies. As discussed above, the annihilation is to a large extent independent of the lattice effects which determine the electron effective mass and Fermi energy. Lithium is a typical example of a case where the values of the Fermi energy determined from soft x-ray emission ((4.2 ± 0.3) ev)[36] and calculated from the energy band band theory (3.4 ev)[37] differ appreciably from that calculated on the basis of the Sommerfeld theory (4.75 ev).

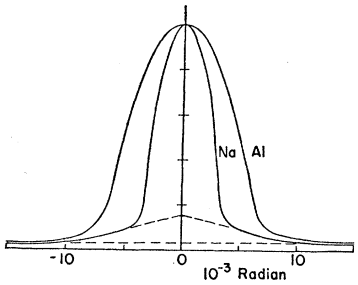

FIG. 7. (After Lang, DeBenedetti, and Smoluchowski). Two-photon angular correlation for sodium and aluminum. The lower dashed line indicates background intensity.

TABLE II. Unit electron sphere radius (in Bohr radii) and parabolic cut-off angle (in milliradians) for several metals.

$r_s=1.384(A/\rho z)^{\frac{1}{3}}$; $\theta_0=13.99/r_s$

Met.	Atomic wt A	Sp. Gr. ρ	Val. z	Rad. r_s	Ang. θ_0
Na	23.0	0.971	1	3.97	3.52
Mg	24.3	1.74	2	2.65	5.28
Al	27.0	2.70	3	2.07	6.75
Si	28.1	2.42	4	1.97	7.10
Cu	63.6	8.94	1	2.66	5.25

Work which clearly exhibits the parabolic distribution was published by Stewart[38] and by Lang, DeBenedetti, and Smoluchowski.[39] Figure 7 has been prepared from the Na and Al curves presented by the latter group of authors. As is evident, the cut-off angles are in good agreement with the values listed in Table II for Na and Al, of 3.52 milliradians and 6.75 milliradians, respectively. Mg is an intermediate case and has also been measured by both Stewart and DeBenedetti *et al.* Both researchers find agreement with the value of 5.28 milliradians (also listed in Table II). The additional element from this same row of the periodic table, silicon, is a semiconductor. The small energy gap of less than one electron volt indicates, however, that the electrons are sufficiently loosely bound that the Bloch waves are more like those in a metal than in an insulator. One should thus expect a parabolic two-photon angular correlation for the semiconductors rather than, say, the triangular distribution found for the alkali halides and discussed in the preceding section.[40] A parabolic distribution in germanium has been reported by Lang and DeBenedetti. Although no work has yet been reported

[35] R. E. Green and A. T. Stewart, Phys. Rev. **98**, 486 (1955).

[36] H. W. B. Skinner, Phil. Trans. Roy. Soc. (London) **A239**, 95 (1940).

[37] See reference 10, p. 440.

[38] A. T. Stewart, Phys. Rev. **99**, 594(L) (1955).

[39] Lang, DeBenedetti, and Smoluchowski, reference 33.

[40] Similar remarks apply to positron annihilation in superconductors, which should not differ in any appreciable respect from annihilation in normal conductors. For references to the experimental literature see B. Green and L. Madansky, Phys. Rev. **102**, 1014 (1956).

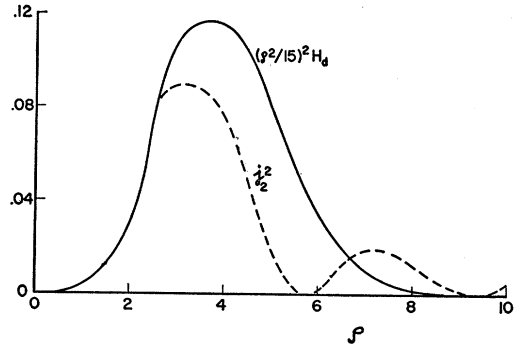

FIG. 8. Comparison of approximate function (solid curve) with exact function (dashed curve) for d-electron annihilation.

on silicon the cut-off angle is listed in Table II and should fall at 7.10 milliradians, according to Eqs. (17) and (18) above.

Returning to Fig. 7 one notes that there are small tails to the parabolic distributions for both Na and Al. In Na the tails are roughly linear and suggest the outermost portion of the triangular-type distribution found in the alkali halides. Such a distribution could result from the incomplete expulsion of the positron wave function from the positive ion cores. The finite overlap of the spherically symmetric positron wave function with the radial wave functions of the core electrons gives rise to a radial factor in the wave-function product which has a peak in the neighborhood of the ion radius, just as in the case of the alkali halides. The noble gas configuration of the Na^+ ion is the same as that of F^-. Since the cut-off angle in LiF is 10.6 milliradians, one expects about the same for the core annihilation in Na (the tendency for the maximum in the wave function product to occur at larger radii for a nonbound positron may compensate for the smaller radius of the positive ion). The cut-off angle of 10 milliradians, determined from Fig. 7, seems to be consistent with this picture. In Fig. 7 the linear tails have been extended inward. The area of the resulting triangle, enclosed by the dashed lines, is then to be attributed to core annihilation, which consequently would amount to about 25% of the total annihilation rate. Although this appears on the surface to be fairly natural explanation of the Na tails, it cannot be applied to Al, where the tails do not seem to have the linear property. It is clear from first principles that some core annihilation must take place in these metals, but a rough estimate indicates that considerably less than 25% of the annihilation rate can arise in this way. We are therefore led to consider additional effects which can give rise to the tails. But before proceeding it is of interest to consider the noble metals, for which, because of the large core consisting of ten d electrons, core annihilation can be expected to be more important than in Na and Al.

The annihilation of a positron in a spherically asymmetric state with a filled atomic d shell can be treated in the same way as the s and p annihilation. As in the preceding section, we make the expansion of $e^{-i\mathbf{k}\cdot\mathbf{r}}$ in terms of spherical harmonics. If the z axis is chosen along the direction of $\mathbf{k}$ only the $m=0$ substate can contribute. Integrating out the Fourier transform gives a probability function proportional to $(j_2(ka))^2$ where the wave function product has been assumed to peak fairly sharply at $r=a$. As in Sec. IIB, we fit the function for small $\rho=ka$ by the following convenient approximation:

$$(j_2(\rho))^2\equiv[(3/\rho^3-1/\rho)\sin\rho-(3/\rho)\cos\rho]^2$$
$$=(\rho^2/15)^2(1-\rho^2/7+\cdots)\approx(\rho^2/15)^2\exp(-\rho^2/7)$$
$$\equiv(\rho^2/15)^2H_d(\rho).$$

This approximation is illustrated in Fig. 8 and is somewhat less accurate than the corresponding approximations in the case of s and p annihilation, since the maximum falls at a larger value of ρ, and thus further away from the region of good fit. The greater height of the approximate curve is of no consequence here, but it will be noted that the half-peak value of ρ is a factor of 1.06 too large on the rising side of the curve and 1.19 too large on the descending side. A better fit is therefore given by reducing the horizontal scale in the plot of $(\rho^2/15)^2Hd(\rho)$ by 1.12, the geometrical mean of the above factors. It will be further noted that the plot of $(\rho^2/15)^2Hd(\rho)$ fails to reproduce the secondary maxima in $(j_2(\rho))^2$. As explained in Sec. IIB, this is an entirely satisfactory feature of this type of approximation.

In order to compare with experiment it is necessary to integrate over two of the Cartesian components of $\mathbf{k}$. Proceeding as in IIB, but making the slightly different change of variable $\zeta=k_za/\sqrt{7}$, $u=(k_x^2+k_y^2)a^2/7$, the distribution function for k_z is proportional to

$$f(\zeta)=\tfrac{1}{2}\int_0^\infty(\zeta^2+u)^2\exp(-\zeta^2-4)du$$
$$=(1+\zeta^2+\zeta^4/2)\exp(-\zeta^2). \qquad (21)$$

This function is plotted in Fig. 9 and is very flat for values of ζ less than unity. The half-maximum value is $\zeta=1.64$, corresponding, (including the scale factor of 1.12), to $k_z=3.88$, or to an angle of

$$\theta_d=14.98/a, \qquad (22)$$

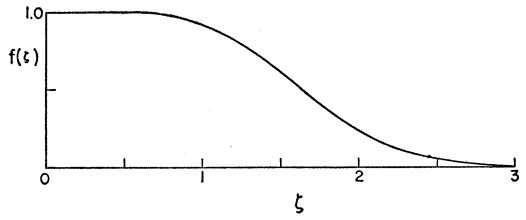

FIG. 9. d-shell two-photon angular correlation as a function of $\zeta=(amc/\sqrt{7}\hbar)\cdot\theta$, where θ is the projected angle between the directions of the annihilation photons and a is the d-shell radius.

where a is measured in Angstroms and θd in milliradians.

Figure 10 shows the two-photon angular correlation curve for copper (prepared from the paper by Lang *et al.*[39]), and seems to exhibit d annihilation with the above properties. According to Table II, the s electrons should have a cut-off angle of 5.25 milliradians. A parabola fitting the curve at small angles has been extended out to this angle and accounts for about one-third of the total number of counts. The remaining counts are spread out over a distribution which is flat at small angles (as shown by the dashed line), and which has a falloff at larger angles similar to that in Fig. 9. The half-maximum angle of this broad component is 8.68 milliradians, corresponding to a core radius, according to Eq. (22) of $a=1.72$ A. This value is considerably larger than the half-nearest neighbor spacing of 1.27 A, which is an overestimate of the ion radius. This latter value would yield, according to Eq. (22) a half-maximum angle of 12.8 milliradians, in significant disagreement with Fig. 10.

One is forced to the somewhat disappointing conclusion that, even in the metals with relatively the largest cores, the tails in the two-photon angular correlation do not directly reveal features of the cores themselves, but instead must be due to a breakdown of the simplifying approximations introduced above. We turn first to the excluded volume effect, since DeBenedetti *et al.*[41] have emphasized that it can be expected to be particularly important for the noble metals. Let the true positron wave function in the metal be $\psi(\mathbf{x})$. In the interstitial region $\psi(\mathbf{x})$ is a constant, which we take to be unity, but inside the positive ions it drops to zero. Being an eigenfunction of the crystal momentum operator with eigenvalue zero, $\psi(\mathbf{x})$ is a real positive function of $\mathbf{x}$ and has the "Swiss cheese" structure rereferred to above. Since the wave-function product is now no longer a plane wave, $\mathbf{k}=\mathbf{K}$ is no longer required for the annihilation with a electron of crystal momentum $\mathbf{K}$. This relation must now be generalized to $\mathbf{k}=\mathbf{K}+\boldsymbol{\kappa}$, where $\boldsymbol{\kappa}$ is a reciprocal lattice vector. It is convenient to write the wave-function product as

$$\psi(\mathbf{x})e^{i\mathbf{K}\cdot\mathbf{x}}=e^{i\mathbf{K}\cdot\mathbf{x}}-(1-\psi)e^{i\mathbf{K}\cdot\mathbf{x}},$$

where the first term can annihilate only into $\mathbf{k}=\mathbf{K}$, and the second term alone contributes for $\mathbf{K}\neq 0$. Here we continue to approximate the Bloch waves by plane waves, since $\psi(\mathbf{x})$ is assumed to vanish in the regions where this is not a good approximation. A calculation similar to that carried out in Sec. IIB shows that the probability of annihilation into $\mathbf{k}=\mathbf{K}+\boldsymbol{\kappa}$, for $\boldsymbol{\kappa}\neq 0$, is proportional to the absolute square of

$$f_{\boldsymbol{\kappa}}=\frac{1}{v_0}\int_{v_0}(1-\psi)e^{-i\boldsymbol{\kappa}\cdot\mathbf{x}}d^3\mathbf{x},$$

where the integration is now over the unit cell of volume v_0 centered at one of the positive ions. This can be simplified by using the expansion given in IIB of the factor $\exp(-i\boldsymbol{\kappa}\cdot\mathbf{x})$. Since the function $(1-\psi)$ is spherically symmetric, only the $l=0$ term, $j_0(\kappa r)$, contributes, where $r=|\mathbf{x}|$. The above expression becomes, if we carry out an integration by parts and use the identiy[42] $-j_0'=j_1$,

$$\begin{aligned}f_{\boldsymbol{\kappa}}&=\frac{4\pi}{v_0}\int_0^\infty(1-\psi)\frac{\sin\kappa r}{\kappa r}r^2dr\\&=-\frac{4\pi}{v_0\kappa}\frac{\partial}{\partial\kappa}\int_0^\infty(1-\psi)\cos\kappa r\,dr\\&=-\frac{4\pi}{v_0\kappa}\frac{\partial}{\partial\kappa}\int_0^\infty\frac{d\psi}{dr}\cdot\frac{\sin\kappa r}{\kappa r}dr\\&=\frac{4\pi}{v_0}\int_0^\infty r^3\frac{d\psi}{dr}\cdot\frac{j_1(\kappa r)}{\kappa r}dr.\end{aligned}\tag{23}$$

It has been permissible to extend the radial integration to infinity since the factor $(1-\psi)$ vanishes outside the core. ψ rises rapidly from zero to unity at roughly the core radius a. The approximation $d\psi/dr\approx\delta(r-a)$ then leads to

$$|f_{\boldsymbol{\kappa}}|^2\approx(v_c/v_0)^2G_p(\kappa a)\approx(v_c/v_0)^2H_p(\kappa a)\tag{24}$$

where $v_c=4\pi a^3/3$, the excluded volume, equals roughly the core volume. $G_p(\kappa a)$ is the function defined in Sec. IIB and is approximated by the Gaussian $H_p(\kappa a)=\exp[-(\kappa a)^2/5]$ (see Fig. 5).

The probability distribution for $\mathbf{k}=\mathbf{K}+\boldsymbol{\kappa}$ is obtained by folding the distribution for $\mathbf{K}$ (the Fermi sea) into the above distribution for $\boldsymbol{\kappa}$. Although $\boldsymbol{\kappa}$ is confined to points in the reciprocal lattice, for the present very rough purpose we can consider it as a continuous variable. The resulting folded distribution is also

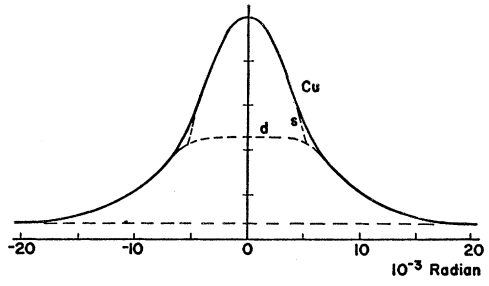

FIG. 10. (After Lang, DeBenedetti, and Smoluchowski). Two-photon angular correlation for copper. The portion of the distribution above the upper dashed line is attributed to annihilation of conduction electrons, uncorrected for the excluded volume effect. The lower portion is attributed to expulsion of the positron wave function from the region enclosed by the d shell. The lower dashed line indicates background.

[41] Reference 18. Our discussion follows that given there rather closely.

[42] See reference 20, p. 78.

roughly a Gaussian, resulting in the same Gaussian for the distribution of the z component of momentum. The half-maximum angle for this distribution is

$$\theta_c=(0.692\theta_0^2+51.6a^{-2})^{\frac{1}{2}}, \tag{25}$$

where θ_0 is the parabolic cut-off angle previously defined. All angles are measured in milliradians, while a is in angstroms. Since the experimental curve for copper (after subtracting the parabola—see Fig. 10) also roughly fits a Gaussian, we can use the experimental value of $\theta_c=8.68$ milliradians in conjunction with Eq. (25) to determine a. This yields $a=0.98$ A, a reasonable value. Since $r_sa_0=1.41$ A, it follows that $v_c/v_0=0.34$.

The intensity of the parabola relative to that of the entire distribution provides an independent determination of the core volume. It is easy to show that the ratio of the total number of counts in these two distributions is

$$F_0=(1-2v_c/v_0)/(1-v_c/v_0). \tag{26}$$

By equating this to the experimental value of 1/3 one finds $v_c/v_0=0.40$, in satisfactory rough agreement with the preceding paragraph. Copper thus seems to be a clear case of the excluded volume effect, and this is no doubt true for the other noble metals. It is perhaps also the case for the transition, rare earth, and actinium series metals—all of which have large ion cores. Returning now to the more ideal metals with smaller ion cores, let us try to account for the tails in sodium by the excluded volume effect. The half-maximum angle for the triangular distribution drawn in Fig. 7 is about 5 milliradians. If we replace the triangle by a Gaussian with slope at the points of influection equal to that of the sides of the triangle, the half-maximum angle is larger than that for the triangle by the factor $(2\ln 2)^{\frac{1}{2}}=1.177$. Thus we set $\theta_c=5.9$ milliradians and from Eq. (25) determine $a=1.41$ A. This is larger than the core radius[16] of 0.98 A, but smaller than the unit sphere radius of $r_sa_0=2.10$ A. It follows that $v_c/v_0=0.30$, giving for the fraction of counts in the parabola, according to Eq. (26) only about 57%. The remaining 43% should be attributed to a broad Gaussian on which the parabola sits. This value is excessive and the disagreement between it and the rough earlier estimate of 25% is probably to be attributed to experimental uncertainties in the shape of the tail, which lies fairly close to background. We therefore invert Eq. (26) and solve for v_c/v_0 assuming $F_0=3/4$. This yields the fairly reasonable values of $v_c/v_0=0.20$, $a=1.23$ A, and $\theta_c=6.55$ milliradians. Because of the Coulomb field surrounding a positive ion, it is possible that the positron wave function, considered as a function of decreasing radius, drops essentially to zero before the ion core is reached. In this way the excluded volume can be greater than the core volume. If we however, require a to equal the core radius, then

$$v_c/v_0=0.10, \quad F_0=0.89, \quad \text{and} \quad \theta_c=7.90.$$

This possibility, which would attribute to the excluded volume effect a distribution broader than assumed in the foregoing and containing only 11% of the counts, is not excluded by the measurements of Lang *et al.*, and seems to be indicated by the more recent work of Stewart (see below).

It is an essential property of the excluded volume effect that it simply adds a broad smooth two-photon angular correlation curve to the parabolic curve. The abrupt cutoff of the latter curve is not affected, and hence the composite curve should also show a discontinuity in slope at $\pm\theta_0$. This feature is present (within the experimental resolution of one milliradian) in the curves of Lang *et al.* for Cu and Na (Figs. 10 and 7). If we now however consider Al (Fig. 7), we note a more gradual change in the slope at the junction of the parabola with the tails. Some other failure of the approximations made above, rather than the excluded volume effect, must therefore be the reason for this deviation in Al from the ideal case of annihilation in a degenerate electron gas. The approximation which fails in Al is clearly the neglect of the deviation of the Bloch waves from plane waves. This deviation may be appreciable, even in the interstitial regions, because the Fermi surface in Al overlaps the zone boundaries. The electrons slightly below the Fermi surface can thus be thrown into momentum states slightly above the Fermi surface by interaction with the lattice. The stationary state wave functions, or Bloch waves, are thus mixtures of plane waves. In the momentum representation, the Fermi surface has become very much blurred, resulting in a gradual rather than a sharp parabolic cutoff. This effect shows up especially clearly in some recent work of Stewart. Stewart has achieved sufficiently accurate statistics that he is able to differentiate numerically his experimental data, yielding the distribution function $P(k)$ itself, rather than the integrated quantity

$$P_z(k_z)=\frac{1}{\pi k_0^2}\int\int P((k_x^2+k_y^2+k_z^2)^{\frac{1}{2}})dk_xdk_y.$$

If we denote differentiation of $P(k)$ by $P'(k)$ and introduce $u=k_x^2+k_y^2$, $k=(u+k_z^2)^{\frac{1}{2}}$, we find

$$-\frac{k_0^2}{2k_z}\frac{dP_z}{dk_z}=-\int_0^\infty P'((u+k_z^2)^{\frac{1}{2}})\frac{du}{2(u+k_z^2)^{\frac{1}{2}}}$$

$$=-\int_{k_z}^\infty P'(k)dk=P(k_z). \tag{27}$$

This procedure requires isotropy, in that P is assumed to be a function only of the magnitude of $\mathbf{k}$ and not on its direction. In the ideal case of an electron gas the parabolic function $P_2(k_2)=1-(k_z/k_0)^2$ yields, according to Eq. (27), a step function for P which is unity for $k<k_0$ and vanishes for $k>k_0$. This is of course, simply the occupation function for the Fermi sea.

Stewart's[43] plots of $P(k)$ (in arbitrary units) are shown at the left of Fig. 11. The horizontal axis measures k in units of $2(mc/\hbar)\times10^{-3}=0.274a_0^{-1}$, and the position of k_0 is indicated by a vertical arrow pointed downward. The $P(k)$ curve for Al deviates significantly from the ideal step function, indicating a strong effect of the lattice on the Fermi sea. Na approaches much more closely the ideal step function, which generally should be the case in the monovalent metals. In these the Fermi surface does not yet fill up the first Brillouin zone and it is not possible for the lattice to scatter the electrons out of the Fermi sea while still nearly conserving energy. There is consequently much less mixing in momentum space than in the case of higher valence metals. Stewart's plot of $P(k)$ for copper shows, for example, the same abrupt drop at the Fermi surface as does his plot for sodium. In Cu this step function is superposed with the broad smooth Gaussian arising from the excluded volume effect. Stewart's plots of the function $k^2P(k)$ appear on the right half of Fig. 11 and show the distribution of counts with respect to the magnitude of the momentum transferred to the annihilation photons. These plots serve to magnify the high momentum tails in $P(k)$. The excluded volume effect in copper thereby shows up especially clearly. The very weak tail in sodium indicates that our above figures may overestimate the excluded volume in this metal. A more quantitative theoretical estimate of how large v_c/v_0 should be in Na would require knowledge of the positron wave function ψ. Numerical computations of ψ are in progress[44] for various monovalent metals, using the self-consistent field inside the unit sphere and the boundary condition of vanishing radial derivative at the surface. It is hoped that these computations may throw some additional light on the excluded volume effect, and indirectly may yield some information on the charge distribution in the ion cores from which the positron wave function is expelled.

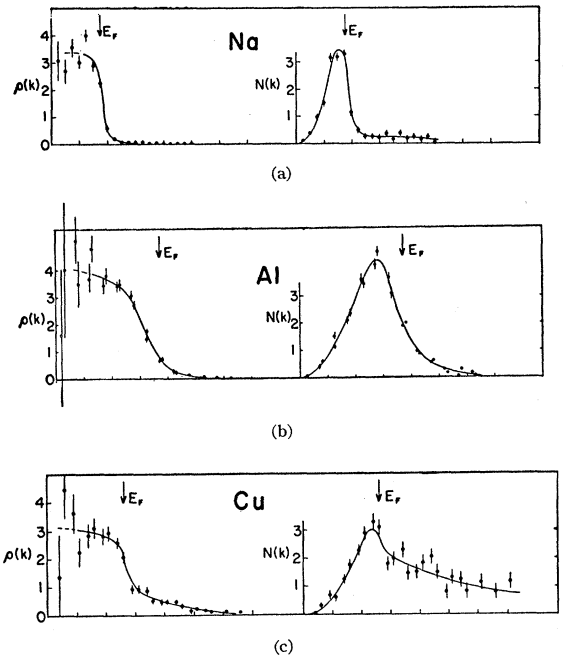

FIG. 11. (After Stewart.) Two-photon angular correlation for sodium, and aluminum, and copper. The notation is explained in the text.

[43] We are much indebted to Dr. Stewart for supplying us with this material in advance of publication.

To summarize this section, the following three effects in metals produce deviations from the ideal parabolic two-photon angular correlation curve:

(1) Excluded volume effect.
(2) Deviation of Bloch waves from plane waves.
(3) Core annihilation.

There is definite evidence for (1) in the noble metals. (2)does not seem to matter in the monovalent metals, but is important in the multivalent metals. There does not seem to be any evidence for (3).

B. Lifetime

In the preceding section the contribution of the conduction electrons to the total annihilation rate of a positron in a metal has been discussed. The two-photon angular correlation measurements make it possible to identify this contribution and the experimental result is that the positrons annihilate essentially only with the conduction electrons. All metals investigated have been found to have the uniformly short lifetime, $\tau=(1.5\pm0.7)\times10^{-10}$ sec.[3,45,46] The total annihilation rate for any metal is therefore roughly

$$\lambda=\tau^{-1}=(6.67\pm3)\times10^{9}\ \text{sec}^{-1}.$$

For studying the annihilation with the conduction electrons the Sommerfeld free electron theory of metals is a useful starting basis. The positive charge is considered to be uniformly smeared out so as to have no effect on the electron motion, except for canceling the average negative charge density of the electrons. In this theory a metal is distinguished only by a certain value of electron density, which is most conveniently specified by the dimensionless unit sphere radius r_s defined in Sec. A. As discussed in the Introduction, the rate of annihilation is proportional to the electron density at the positron. Taking this density equal to n

[44] R. Latter, (private communication).
[45] S. DeBenedetti and H. J. Richings, Phys. Rev. **85**, 377 (1952).
[46] G. E. Minton, [Phys. Rev. **94**, 758 (1954)] reports the longer lifetime of $(2.9\pm0.3)\times10^{-10}$ sec for aluminum, which would decrease all the experimental rates stated below by a factor of two.
Note added in proof.—Dr. Minton informs me (private communication) that in a subsequent measurement with refined apparatus he obtained $(2.4\times0.3)\times10^{-10}$ sec. This value is in good agreement with a recent measurement by Gerholm [T. R. Gerholm, Arkiv Fysik **10**, 523 (1956)], who finds a lifetime of $(2.5\pm0.3)\times10^{-10}$ sec for positrons in aluminum. Gerholm suggests possible sources of a small systematic error in the work of Bell and Graham, which might have made their lifetime values too small by 1.0×10^{-10} sec.

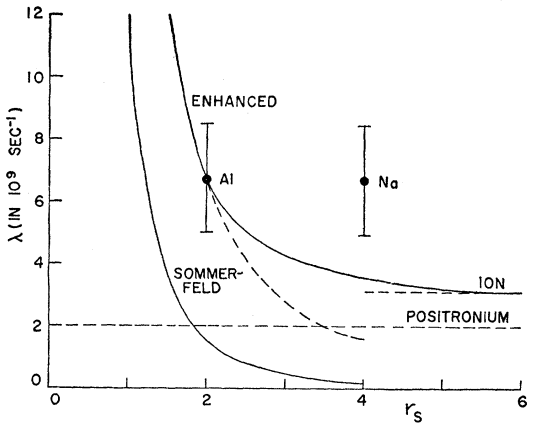

FIG. 12. Comparison of theoretical and experiment values for the annihilation rate of a positron in an electron gas. See text for notation.

and using as a convenient comparison the case of positronium, where the spin-averaged rate is $\lambda_0=\frac{1}{4}(1.25\times10^{-10}\ \text{sec})^{-1}=2.00\times10^{9}\ \text{sec}^{-1}$ and the density is $1/8\pi a_0^3$, we find a conduction-electron annihilation rate of

$$\lambda_{\text{Somm}}=\lambda_0\cdot n(1/8\pi a_0^3)^{-1}$$
$$=\lambda_0\cdot(3/4\pi a_0^3 r_s^3)\cdot 8\pi a_0^3=12 r_s^{-3}\times10^{9}\ \text{sec}^{-1}. \quad (28)$$

The Sommerfeld theory can be expected to apply to real metals only in the cases where the more refined theories indicate a Fermi energy approximately equal to that given by the Sommerfeld theory. This is known to occur only for the group of metals following Ne in the periodic table, *viz.*, Na, Mg, Al, etc. Of these, only the first three seem to have been studied with regard to positron annihilation. The r_s values are 3.97, 2.67, and 2.07, respectively. Thus magnesium is an intermediate case and we shall limit the discussion to the two extreme cases of sodium and aluminum, which represent a range of electron density by a factor of 7.02. Now using Eq. (28) above we find for Na and Al rates which are smaller than the experimental values plotted in Fig. 12 by factors of 36 and 5, respectively. This has generally been considered a serious discrepancy between theory and experiment, particularly in the case of sodium, and is especially evident from the curve labeled "Sommerfeld" in Fig. 12, which shows λ_{Somm} in Eq. (28) plotted *vs* r_s.

This discrepancy is actually more apparent than real, and it is the purpose of this section to show that it can be removed by a straightforward improvement in the Sommerfeld electron theory. The essential shortcoming of the above calculation is that the *average* electron density has been used in computing the annihilation rate, rather than the *actual* density of the electrons at the position of the positron. The actual electron density at the positron is much greater than the average because of the strong Coulomb attraction which the positron exerts on the electrons. The calculation of the extent of this polarization of the electron gas about the positron is inherently a quantum-mechanical many-body problem and must take into account, in addition to the positron-electron attraction, the following three main features: The repulsive Coulomb interactions between the electrons, the Heisenberg uncertainty principle, and the Pauli exclusion principle. The first of these opposes the polarization, since the induced negative charge screens out the positron charge and thus neutralizes the agent causing the polsarization. The uncertainty principle also opposes the polarization by preventing the electron wave functions from collapsing about the positron. The exclusion principle, on the other hand, aids the polarization by permitting short wavelength changes in the electron wave functions (corresponding to the admixture of high-momentum components). The uncertainty and exclusion principles are automatically taken into account in any consistent quantum-mechanical treatment of the problem. It is therefore the Coulomb interaction of the electrons which makes an exact treatment out of the question and an approximate treatment difficult. This interaction is too strong to be dealt with as a perturbation, but can fortunately be transformed away to a large extent by a canonical transformation, as shown by Bohm and Pines.[47] The electron-electron interaction which remains in their theory is a much weaker short-range repulsion which can be satisfactorily handled by perturbation theory.[48] The Bohm-Pines theory can be used in the present problem, and a brief outline of such a treatment is given in the next section. Here we want instead to give a cruder variational calculation of the polarization which nevertheless takes into account all the important effects, and which yields roughly the same result as the more exact treatment.

The screening resulting from the polarization of the electron gas considerably weakens the Coulomb field around the positron, except at very close distances. The effective potential about the positron is therefore quite different from a true Coulomb potential. The long tail of the latter would have an especially strong effect on slow electrons, pulling them into the center of force and causing them to annihilate more rapidly with the positron. The effect of attraction by a pure Coulomb potential is readily calculated and is sufficient to greatly increase the annihilation rate and thereby reduce the discrepancy between theory and experiment. The two-photon angular correlation measurements, however, show no predominant annihilation with slow electrons. One thus has strong experimental evidence for the screening of the positrons, which is similar to the screening of impurity centers in a metal. The Fermi-Thomas statistical model can be used to find the self-

[47] D. Bohm and D. Pines, Phys. Rev. **92**, 609 (1953).
[48] D. Pines, *Solid State Physics* (Academic Press, Inc., New York, 1955), Vol. I, p. 367.

consistent potential about the impurity.[49] In the present problem, however, we need to know primarily the electron density rather than the potentia . For this purpose the statistical model is too crude, yielding, as a matter of fact, the value infinity for the electron density at the positron. An additional difficulty is that the positron, being a light particle, does not set up a central field common to all the electrons. We therefore turn to the following variational approach to the specific problem of finding the density of electrons at the position of the positron.

Consider that all the electron wave functions are modified, relative to the plane waves, by the factors $1+Ce^{-r/a}$, which are practically unity for values of the electron-positron separation r greater than the constant $2a$. The constant C determines the enhancement factor, $(1+C)^2$, of the electron density at the positron. The behavior of a factor of this type as a function of r is illustrated by the curve labeled $|\psi|$ in Fig. 13. Representing the polarization by this factor, with undetermined C and a, we choose as trial wave function

$$\Psi=\varphi_0(\mathbf{x}_0)\Pi_i(1+Ce^{-(\mathbf{x}_i-\mathbf{x}_0)/a})\varphi_i(\mathbf{x}_i),$$

where $\mathbf{x}_0$ and φ_0 are the positron coordinate and wave function, while $\mathbf{x}$ and φ_i are the coordinates and wave functions of the electrons. The φ_i are normalized plane waves corresponding to the various momenta in the Fermi sea. To avoid complications from the nonorthogonality introduced by the electron-positron correlation factors we do not antisymmetrize Ψ. Rather, we follow the less rigorous procedure of including the effect of exchange between electrons of like spin by introducing the exchange hole at a later stage.[50]

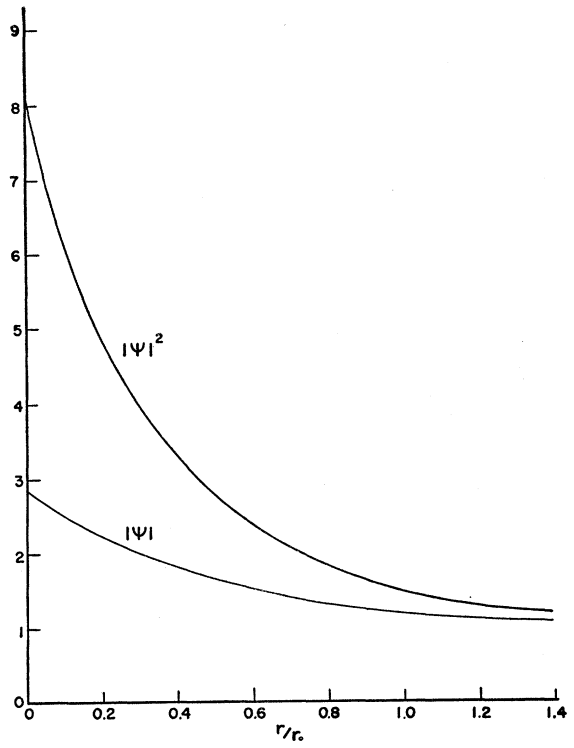

FIG. 13. Wave function and density enhancement factors as functions of the positron-electron separation (in units of the unit sphere radius).

[49] J. Friedel, Advances in Phys. 3, 446 (1954), and references therein.

We now determine C and a by minimizing the total energy. Consider first the kinetic energy operator, T_i of the ith electron. Applied to Ψ it gives a term proportional to $T_i(1+Ce^{-|\mathbf{x}_i-\mathbf{x}_0|/a})$, and a cross-term proportional to $\mathbf{k}_i\cdot(\mathbf{x}_i-\mathbf{x}_0)$, where $\mathbf{x}_i$ is the wave vector of the ith electron. Upon calculating the expectation values, the cross-term vanishes in the integration over $\mathbf{x}_i$, while the $T_i\varphi_i(\mathbf{x}_i)$ term yields $\hbar^2k_i^2/2m$. A sum of this over all N electrons gives $\frac{3}{5}NE_0$, where E_0 is the Fermi energy and is independent of C and a. Returning to the part of the kinetic energy involving the correlation factor, we see that the positron kinetic energy operator yields a term just equal to that written down above. [Here we can ignore the cross-terms proportional to $(\mathbf{x}_i-\mathbf{x}_0)\cdot(\mathbf{x}_j-\mathbf{x}_0)$, since they vanish in the integration.] Integrating these two equal terms over the relative coordinate $\mathbf{x}=\mathbf{x}_i-\mathbf{x}_0$ gives

$$\begin{aligned}
&2\int(1+Ce^{-x/a})(-\hbar^2/2m)\nabla_x^2(1+Ce^{-x/a})d^3\mathbf{x}\\
&=2\pi a^3C^2\int\frac{e^{-x/a}}{(\pi a^2)^{\frac{1}{2}}}\left(-\frac{\hbar^2}{2m}\right)\nabla_x^2\frac{e^{-x/a}}{(\pi a^3)^{\frac{1}{2}}}d^3\mathbf{x}\\
&=2\pi a^3C\left(\frac{a_0}{a}\right)^2\int\psi_{100}(x)(-\hbar^2/2m)\nabla_x^2\psi_{100}(x)d^3\mathbf{x}\\
&=2\pi a_0^2aC^2\,\mathrm{ry},
\end{aligned}\tag{28A}$$

where ψ_{100} is the hydrogen ground-state wave function and ry is the rydberg. Since $\sum_i|\varphi_i|^2=n=3/4\pi a_0^3r_s^3$, the expectation value of the total kinetic energy is

$$\langle T\rangle=\tfrac{3}{5}NE_0+\frac{3}{2r_s^3}\frac{a}{a_0}C^2\,\mathrm{ry}.$$

The expectation value of the total potential energy is composed of the positron-electron attractive part $\langle V_{pe}\rangle$, and the electron-electron repulsive part $\langle V_{ee}\rangle$. Both of these parts depend only on the charge density

$$\rho=-ne[(1+Ce^{-x/a})^2-1]=-ne(2Ce^{-x/a}+C^2e^{-2x/a}).$$

The C^2 term in this expression represents a charge distribution confined closely to the region around the positron. It therefore occupies a relatively small total volume and possesses a relatively small total charge. Its contribution to the total potential energy can consequently be neglected provided C satisfies the in-

[50] E. Wigner and F. Seitz, Phys. Rev. 43, 804 (1933).

equality $C^2<2C$ or $C<2$. The effect of this approximation can be seen explicitly in the expression for $\langle V_{pe}\rangle$:

$$\langle V_{pe}\rangle=\int\frac{e\rho}{x}d^3\mathbf{x}=-4\pi ne^2\int_0^\infty(2Ce^{-x/a}+C^2e^{-2x/a})xdx$$
$$=-\frac{3e^2a^2}{r_s^3a_0^3}(2C+C^2/4).$$

The second term is less than one-fourth of the first for $C<2$. Thus, the approximation of neglecting the C^2 term in the charge density limits the accuracy of our work to 25% (in the interval $0\leq C\leq 2$, which, as we shall see, is the interval of greatest interest). With this approximation,

$$\langle V_{pe}\rangle=-\frac{12}{r_s^3}\left(\frac{a}{a_0}\right)^2 C \text{ ry}. \tag{29}$$

The calculation of $\langle V_{ee}\rangle$ is similar. Here we must, however, take into account the exclusion principle, which has been ignored so far, except in that the electrons have been considered to be in different plane wave states φ_i. But electrons of the same spin are also required to be in different eigenstates of the position operator, or in other words, the wave function must vanish when the coordinates of two such electrons are set equal. Our wave function Ψ does not have this property, which is a defect which can be expected to affect mainly the electron-electron interaction. We correct for it by studying the result of properly antisymmetrizing Ψ in the simpler case of no positron present. Then each electron is surrounded by an "exchange hole."[50] The probability of finding two electrons of the same spin at the same place is zero; it is small for all relative separations smaller than a radius of the order of magnitude of the de Broglie wavelength of the electrons at the top of the Fermi sea. Since we are interested in a screening cloud of still smaller dimensions, we can take the exclusion principle into account by considering that only electrons of opposite spin can be present and interact within the screening cloud. Thus, the screening results from the repulsion of two equal charge distributions, corresponding to the two different directions of spin, each of density $\rho/2$. Their mutual Coulomb energy is approximately

$$\langle V_{ee}\rangle=\int\int\frac{\rho(\mathbf{x}_1)\rho(\mathbf{x}_2)}{4|\mathbf{x}_1-\mathbf{x}_2|}d^3\mathbf{x}_1d^3\mathbf{x}_2$$
$$=n^2C^2\int\int e^{-x_1/a}e^{-x_2/a}\frac{e^2d^3\mathbf{x}_1d\mathbf{x}_2}{|\mathbf{x}_1-\mathbf{x}_2|}$$
$$=(2\pi a^3)^2n^2C^2\int\int\frac{e^{-2x_1/2a}}{\pi(2a)^3}\cdot\frac{e^2d^3\mathbf{x}_1d^3\mathbf{x}_2}{|\mathbf{x}_1-\mathbf{x}_2|}\cdot\frac{e^{-2x_2/2a}}{\pi(2a)^3}.$$

The integral appearing here is the same as that encountered in the usual variation treatment of the helium atom,[51] and has the value $5a_0/8a$ ry. Substituting this expression and the expression for n one obtains

$$\langle V_{ee}\rangle=\frac{45}{2r_s^6}\left(\frac{a}{a_0}\right)^5C^2 \text{ ry}. \tag{30}$$

From Eqs. (28A), (29), and (30) the expectation value of the total energy of the system is $3NE_0/5+\mathcal{H}$ ry$/r_s$ where

$$\mathcal{H}=\frac{3}{2r_s}\alpha C^2-12\alpha^2C+\frac{45}{2}\alpha^5C^2. \tag{31}$$

Here we have introduced the dimensionless parameter $\alpha=a/r_sa_0$. We minimize the energy by requiring $\partial\mathcal{H}/\partial\alpha=\partial\mathcal{H}/\partial C=0$. In the differentiation with respect to α the first term of $\mathcal{H}$ gives a negligibly small contribution. Dropping it introduces an error of less than 5% in the value for α. Thus we find

$$\alpha=(16/75)^{\frac{1}{3}}C^{-\frac{1}{3}}. \tag{32}$$

Substitution into Eq. (31) results in an expression which, when minimized with respect to C, yields

$$C=(8/25)2^{\frac{1}{3}}3^{\frac{2}{3}}r_s^{\frac{3}{4}}=0.659r_s^{\frac{3}{4}}. \tag{33}$$

Inserting this into Eq. (32) one obtains

$$\alpha=2^{\frac{1}{3}}3^{-\frac{1}{3}}r_s^{-\frac{1}{4}}=0.686r_s^{-\frac{1}{4}}. \tag{34}$$

It is interesting to note that the total displaced charge, calculated from the values given by Eqs. (33) and (34) is independent of r_s and has the value $-2.56e$. It is reasonable that this charge is numerically greater than the inducing positron charge, since the average positron-electron separation is smaller than the average electron-electron separation. Thus the positive charge is able to hold around it an induced negative charge of larger magnitude. The positronium ion (see below) is a simpler example of such a situation. In the present problem there is no doubt a deficiency of electrons in the region surrounding the negative charge cloud, since the system is as a whole electrically neutral. This could be taken into account, perhaps, by using a more refined trial wave function in which the correlation factors were sums of two exponentials.

The value of the optimal energy can now be calculated by substituting from Eqs. (33) and (34) into $\mathcal{H}$, giving $\mathcal{H}=-1.793r_s^{\frac{1}{4}}$. If the total energy of the system is written as $\frac{3}{5}NE_0+\Delta E$, we consequently have

$$\Delta E=-1.793r_s^{-\frac{1}{4}} \text{ ry}. \tag{35}$$

This expression indicates an additional criterion for the validity of the above approach. As r_s is increased, the amount of lowering in the energy which Eq. (35) attributes to the positron-electron correlations passes eventually to zero. This is clearly not correct since in the limit of low electron density the positron will not correlate equally with all the electrons, but will capture

[51] See reference 20, p. 175.

a particular one of them and correlate strongly with it. That is, positronium will be formed, resulting in a lowering in the energy equal to the binding energy of the atom:

$$\Delta E = -E_B = -0.500 \text{ ry}. \tag{36}$$

Equation (35) indicates less binding than this for values of r_s in excess of 5.42. Thus our variational treatment trial wave function is clearly too crude an approximation for low electron densities and should be generalized to allow for different correlation factors C and α for the various electrons.[52] The validity calculation as it stands is limited to values of r_s comfortably below 5.42. This is roughly equivalent to the earlier restriction of $C<2$, which according to Eq. (33) requires $r_s<4.39$.

From the above considerations it is clear that the electron density at the positron will always be at least equal to its value in positronium. At very low electron density the annihilation rate will equal one-fourth that of singlet positronium, since as a result of collisions the positron will be passed on from one electron to another.[53] Thus the momentum distribution of the positronium atom will be just that of the electrons, and the two-photon correlation may still be roughly parabolic (albeit very narrow). The quantum-mechanical description of the ground state in the low density limit involves a superposition of configurations. Each configuration describes separately the positron correlated strongly, (as described by the positronium ground state wave function), with one particular electron of a certain momentum, and uncorrelated with the rest.

Actually, the above statements concerning the positronium atom apply equally well to the system of two electrons bound to a positron—the so-called "positronium ion." The positronium ion is slightly more stable than the atom (by about 0.20 ev[7,54]), and is therefore a more correct low electron density limiting form for a positron in an electron gas than positronium itself. It is clear that electron capture will not stop with the capture of one electron but will proceed until the full quota of two electrons is captured by the positron. Hylleraas,[54] who has carried out a five-parameter variational estimate of the positronium ion binding energy, finds that good results are also obtained with the following two-parameter function which includes, besides screening, only radial correlation:

$$\psi(r_1,r_2) = c_0 e^{-(r_1+r_2)/2}[1+c_2(r_1-r_2)^2] \tag{37}$$

r_1 and r_2 are the distances of the electrons from the positron and are measured in units of a_0/k, where $k=L/2M$, $L=11+156C_2$, $M=8+96C_2$. The normalization constant is $C_0=(1/4\pi)N^{-\frac{1}{2}}$, where $N=4+48C_2$. Hylleraas finds that the expectation value of the total energy of the system is minimized by $c=0.05$, which yields $k=0.734$, $N=6.4$. It is now an easy matter to evaluate the electron density at the positron. We square the wave function, set alternately r_1 and r_2 equal to zero, and integrate over the remaining variable, which we denote by r. This gives

$$2c_0^2\cdot 4\pi\int_0^\infty dr\cdot r^2e^{-r}(1+c_2r^2)^2 = (1+24c_2+360c_2^2)/\pi N = 0.485/\pi,$$

which, including the units of length, corresponds to a density of $8k^3\times 0.485\times(1/8\pi a_0^3)$, or 1.53 times the density in positronium. Hence the annihilation rate in the positronium ion is about 3.06×10^9 sec^{-1} corresponding to a lifetime of about 3.27×10^{-10} sec. The accuracy of these figures is of course limited by the approximate nature of the trial wave function defined by Eq. (37), but should perhaps be good to at least 10–20%.

Since we have fairly reliable expressions for the annihilation rate in the two limits of low and high electron density we can bridge the difficult intermediate region by interpolation. Such a procedure is of course rather arbitrary, but since we are dealing with large effects the resulting accuracy should be sufficient for our purposes. For high densities the annihilation rate is based on Coulomb enhancement of the Sommerfeld rate and is given by $\lambda=12r_s^{-3}(1+C)^2 10^9$ sec^{-1}. Substitution from Eq. (33) gives

$$\lambda = 12(r_s^{-\frac{3}{2}}+0.659r_s^{-\frac{3}{4}})^2\times 10^9 \text{ sec}^{-1}, \tag{38}$$

which is shown plotted as the "Enhanced" curve in Fig. 12. For low densities Eq. (38) no longer applies and λ equals the positronium ion rate, as shown by the horizontal "ion" line in Fig. 12. The positronium rate shown by the lower dashed line, is included for comparison. In drawing the interpolation curve, we have arbitrarily assumed that the intermediate region ex-

[52] Important electron-electron correlation effects also set in at these low densities. See, for example, J. S. Plaskett, Phil. Mag. **45**, 1255 (1945).

[53] The possibility of the existence of positronium in a metal, undergoing continuous exchange of the electron partner, has been mentioned by DeBenedetti and Corben (reference 18, p. 209).

Note added in proof.—The negative result of the experiment by Madansky and Rasetti [L. Madansky and F. Rasetti, Phys. Rev. **79**, 397 (1950)], is often cited as evidence of positronium formation in metals. It is reasoned that the experimental apparatus, which contains an accelerating electric field, can only fail to detect the positrons which diffuse through the metal foils if the positrons leave the foils in the form of neutral positronium atoms. An alternative explanation is, however, that the positrons, in those metals where they remain free, are kept in the foils by the image force at the surface, and never do emerge. This force arises from the polarization of the conduction electrons and lowers the energy of a positron when it is inside the foils by the amount given by Eq. (35). In other words, the positive positron affinities of the metals will always prevent the emergence of free positrons. To decide specifically for any given metal if positronium formation takes place Inequality (1) can be applied. The positronium affinity is difficult to estimate, but the electron affinity is given by the work function of the metal. Recently Gerholm [T. R. Gerholm, Arkiv Fysik **10**, 523 (1956)], has found evidence of a weak "τ_2 component" in aluminum, which he attributes to orthopositronium. This result is difficult to understand on two counts: (1) The high electron density in aluminum yields a positron affinity which is energetically unfavorable for positronium formation. (2) The *ortho*-state, if it is formed, must be quenched by rapid electron exchange.

[54] E. A. Hylleraas, Phys. Rev. **71**, 491 (1947).

tends over the interval $2 \leq r_s \leq 5.5$ and have tangentially fitted a smooth curve at the end points to the high and low density curves. The resulting curve, shown as a bold line in Fig. 12, is within the experimental error of the measured rates for Al but somewhat outside for Na. Until the experimental errors are reduced we conclude that there is no basic difficulty involved in understanding the observed fast rates of annihilation with the conduction electrons in metals. The low and intermediate density range is, however, clearly in need for much more careful study than that given here.

A word should perhaps be added concerning the less ideal metals in which the effect of the ion lattice is more pronounced and the Fermi energy differs from that calculated on the basis of a degenerate electron gas. Applying the Sommerfeld theory is less justified in these metals than in Na and Al, but it may still be useful to do so. It is particularly interesting to consider the other alkali metals. These cover a fairly wide range of electron densities,[55] with the highest density given by lithium, for which $r_s=3.22$, and the lowest density by cesium, for which $r_s=5.57$. Potassium is intermediate, with $r_s=4.87$. The positron lifetime has been measured in Li and K and found to be the same as in Na.[56] An especially interesting extreme case of low electron density is cesium. With its large r_s value, cesium[57] has an electron density 2.69 times smaller than that of sodium, and falls just within the low density region of Fig. 12, where a conduction electron annihilation rate of 3×10^{-9} sec^{-1} can be expected.

C. Coulomb Effects

A variational approach such as that used in the preceding section can only account for the gross features of the positron annihilation in metals. To describe the finer points, such as the dependence of annihilation cross section on electron momentum, it is necessary to have a detailed theory of metals which includes the important effects of the Coulomb interactions. Such a theory, the Bohm-Pines electron-plasma theory,[47,48] exists only for the idealized model of a gas of electrons in a uniform smeared out background of positive charge. This abstraction exhibits the most important features of the metals, however, and will be dealt with exclusively in this section. Our treatment will be limited to relatively high electron densities where the Coulomb interactions may be treated as perturbations. The purpose of the present work is to show that the Coulomb field around the positron should result in not only the enhancement of the annihilation rate discussed in B, but also in a small probability for excitation of a plasma oscillation upon annihilation of the positron. It does not seem feasible to observe this effect experimentally, since it would require exceedingly precise measurement of the energy of the annihilation photons. There is, however, evidence for a similar effect in the x-ray emission of metals. The close relationship of positron annihilation and x-ray emission is discussed in Sec. D below.

In order to compute the positron-annihilation behavior of an electron gas it is necessary to calculate the stationary state wave functions of the system to sufficient accuracy, including the very vital Coulomb interactions. Bohm and Pines succeed in doing this with a canonical transformation which removes the strong long-range part of the Coulomb interactions, leaving a short range part which is sufficiently weak to be treated as a perturbation. The stationary state wave functions, under neglect of the short range interactions, are particularly simple in the Bohm-Pines representation. They are Slater determinants of plane waves times Hermite functions of the plasma oscillator variables. If a positron is present in the electron gas it is necessary to include its interactions with the electrons. The resulting wave function for the coupled system can then be expressed in the usual Schrödinger representation, by inverting the Bohm-Pines transformation. From this wave function the electron density at the positron could be obtained, and consequently the lifetime. More detailed properties, such as the annihilation rate for various electron momenta could of course also be obtained in this way.

A more convenient procedure than that outlined in the preceding paragraph is to work entirely in the Bohm-Pines representation, by carrying out the canonical transformation on the annihilation operators, as well as on the Hamiltonian.[58] Denoting the operator which annihilates an electron of momentum $\hbar\mathbf{k}$ by $a_\mathbf{k}$, we make the Bohm-Pines transformation and obtain

$$a_\mathbf{k}^{\mathrm{BP}}=\exp(-iS/\hbar)a_\mathbf{k}\exp(iS/\hbar)\cong a_\mathbf{k}-\frac{i}{\hbar}[S,a_\mathbf{k}], \quad (39)$$

where we neglect commutators of order higher than the first. The operator S, in the notation of second quantization is

$$S=-\frac{ie}{m}\left(\frac{2\pi\hbar^3}{V\omega_p{}^3}\right)^{\frac{1}{2}}\sum_{\kappa<k_c}\sum_{\mathbf{K}}\boldsymbol{\varepsilon}_\kappa\cdot(\mathbf{K}-\boldsymbol{\kappa}/2)\times(A_\kappa a_\mathbf{K}{}^* a_{\mathbf{K}-\mathbf{k}}-A_\kappa{}^* a^*{}_{\mathbf{K}-\kappa}a_\mathbf{K}).$$

Here we have made some rather drastic simplifications of the expression given by Bohm and Pines.[59] V is the volume of quantization, ω_p the plasma frequency,

[55] These values have been taken from a table appearing in the following article on electron interactions in metals: D. Pines, Phys. Rev. **92**, 626 (1953).

[56] S. DeBenedetti and H. J. Richings, Phys. Rev. **85**, 377 (1952).

[57] Lifetime measurements on this metal are in progress by B. Green and L. Madansky (private communication).

Note added in proof.—Dr. Madansky informs me that a preliminary measurement yielded a lifetime of $(3.7\pm0.5)\times10^{-10}$ sec, and consequently an annihilation rate of $(2.7\pm0.4)\times10^{9}$ sec^{-1}. This rate is significantly lower than that for the other metals, and just agrees, within the experimental error, with the annihilation rate of the positronium ion.

[58] The author thanks Professor Pines for helpful suggestions on this point.

[59] Reference 47, p. 617.

$\hbar k_c$ the cut-off momentum, A_κ and A_κ^* the annihilation and creation operators for a plasmon[60] of momentum $\hbar\boldsymbol{\kappa}$, and $\boldsymbol{\varepsilon}_\kappa$ is the unit vector along the direction of $\boldsymbol{\kappa}$. Using the commutation relation

$$[a_{\mathbf{k}'}{}^* a_{\mathbf{k}''}, a_{\mathbf{k}}] = -\delta_{\mathbf{k}'\mathbf{k}} a_{\mathbf{k}''},$$

we split Eq. (39) into

$$a_{\mathbf{k}}{}^{\mathrm{BP}} = a_{\mathbf{k}} + a_{\mathbf{k}}' + a_{\mathbf{k}}'',$$

where

$$a_{\mathbf{k}}' = +\frac{e}{m}\left(\frac{2\pi\hbar}{V\omega_p{}^3}\right)^{\frac{1}{2}} \sum_{\kappa<k_c} \boldsymbol{\varepsilon}_\kappa \cdot (\mathbf{k}-\boldsymbol{\kappa}/2) A_\kappa a_{\mathbf{k}-\kappa}, \quad (40)$$

$$a_{\mathbf{k}}'' = -\frac{e}{m}\left(\frac{2\pi\hbar}{V\omega_p{}^3}\right)^{\frac{1}{2}} \sum_{\kappa<k_c} \boldsymbol{\varepsilon}_\kappa \cdot (\mathbf{k}+\boldsymbol{\kappa}/2) A_\kappa{}^* a_{\mathbf{k}+\kappa}. \quad (41)$$

The second of these operators has the interesting property that it simultaneously annihilates an electron and creates a plasmon. That such an event should occur is not surprising since the annihilating electron leaves a hole in the charge distribution. The surrounding electrons tend to rush into this hole but their inertia carries them too far, resulting in a plasma oscillation.

The probability of such an event as described above relative to the normal mode of decay can easily be estimated by considering the special case of $\mathbf{k}=0$. Then, according to Eq. (41), the matrix element for excitation of a plasmon and simultaneous annihilation of an electron, both of momentum $\hbar\boldsymbol{\kappa}$, is $-(e/2\hbar m)\cdot(2\pi\hbar^3/V\omega_p{}^3)^{\frac{1}{2}}\cdot\boldsymbol{\kappa}$. The total probability of plasmon excitation is found by summing over $\boldsymbol{\kappa}$:

$$P = (\pi e^2\hbar/2m^2\omega_p{}^3 V) \sum_{\kappa<k_c} \kappa^2$$

$$= \frac{\pi e^2\hbar}{2m^2\omega_p{}^3 V}\cdot\frac{4\pi V}{8\pi^3}\int_0^{k_c} \kappa^4 d\kappa^4 = \frac{2\beta^5}{5\pi}\cdot\frac{E_0\ \mathrm{ry}^2}{(\hbar\omega_p)^3}\cdot(a_0 k_0)^3. \quad (42)$$

E_0 is the Fermi energy and $\beta = k_c/k_0$, where $\hbar k_0$ is the Fermi momentum. Equation (18) and the corresponding electron gas expressions $E_0 = 3.67\ \mathrm{ry}/r_s{}^2$ and

$$\hbar\omega p = 3.46\ \mathrm{ry}/r_s{}^{\frac{3}{2}} \quad (43)$$

reduce Eq. (42) to

$$P = 0.0795\beta^5/(r_s)^{\frac{1}{2}}. \quad (44)$$

Since β is at most of the order of unity, the probability for this mode of plasmon creation can never exceed a few percent.[61] Although Eq. (44) holds only for the case of no interaction between the positron and the electron gas it seems likely that the probability of this mode of plasmon creation is small also in the case of interaction. Therefore we neglect the $a_{\mathbf{k}}''$ term of $a_{\mathbf{k}}{}^{\mathrm{BP}}$ in the subsequent work below.

The effect of the $a_{\mathbf{k}}'$ term of $a_{\mathbf{k}}{}^{\mathrm{BP}}$ depends on the density of plasmons in the electron gas resulting from the interaction with the positron. This can be estimated from earlier work[62] on the analogous problem of plasmon creation by an incident fast electron. Here, although the positron is at rest and can only create virtual plasmons, the matrix element for the process is the same, except for sign, as that given there in Eq. (5):

$$H_\kappa' = -(2\pi e^2\hbar\omega_p/V\kappa^2)^{\frac{1}{2}}. \quad (45)$$

The energy required to create a plasmon in the state of momentum $\hbar\boldsymbol{\kappa}$ is $\hbar\omega_p$. (Here we neglect both the dispersion of the plasma oscillations and the recoil energy of the positron.) The probability amplitude for this state, according to first-order stationary state perturbation theory, is

$$c_{\boldsymbol{\kappa}} = H_\kappa'/(-\hbar\omega_p) = (2\pi e^2/V\kappa^2\hbar\omega_p)^{\frac{1}{2}}, \quad (46)$$

so that the total probability of finding a plasmon in the ground state of the coupled system is

$$P' = \sum_{\kappa<k_c} |c_\kappa|^2 = \frac{4\pi V}{8\pi^3}\int_0^{k_c} |c_\kappa|^2\kappa^2 d\kappa$$

$$= e^2\beta k_0/\pi\hbar\omega_p = \beta^2 = r_s/8. \quad (47)$$

The last two expressions were obtained from Eqs. (18), (43), and Pines'[63] equation

$$\beta = 0.353(r_s)^{\frac{1}{2}} \quad (48)$$

for the cut-off parameter. The experimental work of Watanabe[64] and the theoretical work of Quinn and Ferrell[65] indicate that plasmons exist for wavelengths 20–40% shorter than Pine's cut-off wavelength. This difference is, however, not enough to alter significantly the present semiquantitative results. For the sake of convenience and simplicity we continue to use Pines' expression.

---

[60] We follow D. Pines in using this term to denote the quantum of energy associated with a plasma oscillation: D. Pines, Revs. Modern Phys. **28**, 184 (1956), this issue.

[61] In reporting this result earlier, (R. A. Ferrell, Bull. Am. Phys. Soc. Ser. II, **1**, 138 (1956)), it was stated that this effect increases the total annihilation rate in the case of no interaction between the positron and the electron gas. This is, however, not correct, since the second-order terms neglected in Eq. (39) will cancel part of the first term, thereby compensating for the contribution associated with plasmon creation. In general, if Ψ is the ground state of the electron system and Ψ_f the various final stationary states in which it can be left after annihilation then the rate of transfer of momentum $\hbar\mathbf{k}$ to the annihilation photons is proportional to $\Sigma_f|(\Psi_f, a_{\mathbf{k}}\Psi)|^2 = (a_{\mathbf{k}}\Psi, a_{\mathbf{k}}\Psi) = (\Psi, \mathfrak{N}_{\mathbf{k}}\Psi)$, where $\mathfrak{N}_{\mathbf{k}} = a_{\mathbf{k}}{}^* a_{\mathbf{k}}$ is the occupation operator for the plane wave of momentum $\hbar\mathbf{k}$. The total rate is proportional to

$$\Sigma_{\mathbf{k}}(\Psi, \mathfrak{N}_{\mathbf{k}}\Psi) = (\Psi, \mathfrak{N}\Psi) = N(\Psi,\Psi) = N,$$

since Ψ is an eigenfunction of the total number operator $\mathfrak{N} = \Sigma_{\mathbf{k}}\mathfrak{N}_{\mathbf{k}}$ with eigenvalue equal to the total number of electrons, N. The total annihilation rate is thus independent of Ψ and the interactions which determine it. We wish to thank Professor W. Kohn for discussion on this point.

[62] R. A. Ferrell, Phys. Rev. **101**, 554 (1956).

[63] Reference 48, Eq. (6.8).

[64] H. Watanabe, J. Phys. Soc. Japan **11**, 112 (1956).

[65] J. J. Quinn and R. A. Ferrell, Bull. Am. Phys. Soc. Ser. II, **1**, 44 (1956), and paper to be submitted to *The Physical Review*.

The first term of a_k^{BP} can annihilate an electron and leave a real plasmon in the final state. The rate for this process is P' times the Sommerfeld rate. The latter is, however, many times smaller than the actual total annihilation rate. The relative probability that a positron will leave a plasmon behind after it annihilates is therefore, for the present consideration, negligibly small. Evidence for such a weak effect in x-ray emission will be discussed in the next section. Another effect of the virtual plasmons comes from their annihilation by the a_k' term of a_k^{BP}. The state of a zero momentum electron hole and no plasmon is obtained by applying $b_{-\kappa}a_\kappa'$, where $b_{-\kappa}$ is the positron annihilation operator, to the part of the ground state wave function containing a plasmon and recoiling positron of momenta $\pm\hbar\kappa$, respectively. The total coherent amplitude of this final state, arising from the long-range interactions of the positron with the electron gas, is

$$c_{1.r.}=\frac{e}{2m}\left(\frac{2\pi\hbar}{V\omega_p{}^3}\right)^{\frac{1}{2}}\sum_{\kappa<k_c}\kappa c_\kappa. \tag{49}$$

It is a straightforward calculation to substitute for c_κ from Eq. (46) and use the electron gas expressions of Eqs. (18) and (43) to reduce Eq. (49) to $c_{1.r.}=0.1392\beta^3$. According to Eq. (48), β is the order of one-half in the range of electron densities of interest, so that the long-range coherent contribution to the annihilation is only of the order of a few percent.

As shown in the preceding paragraphs, plasma effects in the annihilation process are relatively minor. We now deal with the short range interaction of the positron with the individual electrons. This interaction, except for sign, is the same as that between pairs of electrons. The latter is expressed by the potential function

$$H_{s.r.}(\mathbf{r})=\frac{e^2}{r}\left[1-\frac{2}{\pi}Si(k_cr)\right]=\sum_{k>k_c}\frac{4\pi e^2}{Vk^2}e^{i\mathbf{k}\cdot\mathbf{r}} \tag{50}$$

where $\mathbf{r}$ is the relative coordinate of the pair of electrons. The Si function is tabulated by Jahnke and Emde[65a] and $H_{s.r.}$, the short-range part of the Coulomb potential, is plotted by Bohm and Pines.[66] Let us consider annihilation with the electron in the Fermi sea of momentum $\hbar\mathbf{k}_1$. This state is indicated schematically by the "zero-order" diagram of Fig. 14. The dot at the center of the diagram symbolizes the positron of zero momentum. The effect of the interaction is shown in the lower half of Fig. 14. The left-hand diagram exhibits a virtual collision between the positron and electron, resulting in an exchange of momentum $\hbar\mathbf{k}$. Only exchanges which take the electron outside the Fermi sea are permitted by the Pauli exclusion principle. The matrix element for such a collision is, according to Eq. (50), (with a change in sign), $-4\pi e^2/Vk^2$, while the energy of excitation is $(\hbar^2/2m)(k^2+|\mathbf{k}_1+\mathbf{k}|^2-k_1^2)=(\hbar^2/m)(k^2+\mathbf{k}\cdot\mathbf{k}_1)$. Introducing the positron and electron coordinates, $\mathbf{x}_0$ and $\mathbf{x}_1$, the wave function of the pair can be written, to first order, as

$$\Psi(\mathbf{x}_0,\mathbf{x}_1)=\Psi_0+\Psi_1$$
$$=\Psi_0+\frac{4\pi}{Va_0}\cdot\sum_{\substack{k>k_c\\|\mathbf{k}_1+\mathbf{k}|>k_0}}\frac{e^{-i\mathbf{k}\cdot(\mathbf{x}_1-\mathbf{x}_0)}}{k^2(\mathbf{k}^2+\mathbf{k}\cdot\mathbf{k}_1)}\Psi_0. \tag{51}$$

Ψ_0 is the zero-order product of plane waves for the positron and electron, and the factor $e^{i\mathbf{k}\cdot(\mathbf{x}_1-\mathbf{x}_0)}$ converts it into the first-order state indicated in Fig. 14.

Since Ψ_0 is a common factor of the right-hand member of Eq. (51), it follows that the effect of the Coulomb attraction between the positron and electron is simply to multiply the wave function by a factor which enhances the probability of finding the electron in the vicinity of the positron. Explicit calculation of this correlation factor, which we write simply as Ψ/Ψ_0, is easy for the special case of $\mathbf{k}_1=0$. Carrying out the integration in Eq. (51) and denoting the separation of the pair by r, one finds

$$\Psi/\Psi_0=1$$
$$+\frac{r_s}{6.02}\left[\frac{\sin k_0r}{k_0r}+\cos k_0r-k_0r\left(\frac{\pi}{2}-Si(k_0r)\right)\right]. \tag{52}$$

Figure 15 contains plots of this function for $r_s=2$ and $r_s=4$. The $r_s=4$ curve very much resembles the corresponding curve of Fig. 13, which was obtained from the variational treatment. It will be noted that the present curve contains the refinement that, outside the immediate vicinity of the positron, the enhancement factor drops below unity so as to give a more correct value for the total screening charge.

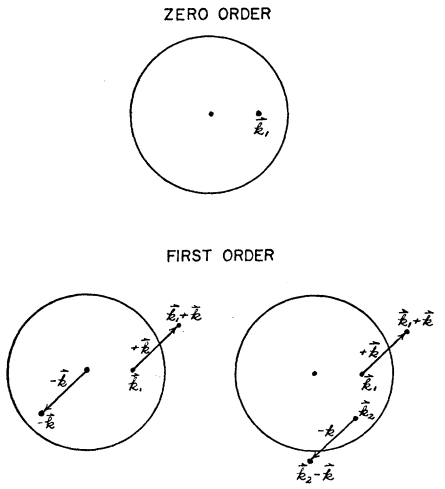

FIG. 14. Momentum diagram of zero-order and first-order states in perturbation theory.

[65a] Reference 21, pp. 1–9.
[66] Reference 47, Fig. 1.

The factor by which the annihilation is enhanced over the Sommerfeld rate is

$$|\Psi|^2/|\Psi_0|^2|_{r=0}=(1+Ck_1)^2,$$

where according to Eq. (51),

$$Ck_1=\frac{r_s}{3.01}\cdot\frac{1}{4\pi}\int\int\int_{\substack{\kappa>\beta\\ |\mathbf{k}_1+\boldsymbol{\kappa}|>1}}\frac{d^3\kappa}{\kappa^2(\kappa^2+\boldsymbol{\kappa}\cdot\mathbf{k}_1)}. \tag{53}$$

Here all the momentum vectors are measured in units of the Fermi momentum. The case $\mathbf{k}_1=0$ is again particularly simple yielding $C_0=r_s/3.01$. This result, which can also be obtained immediately from Eq. (52) by setting $r=0$, enhances the Sommerfeld rate by the factors 2.77 and 5.42 for $r_s=2$ and $r_s=4$, respectively. The corresponding values of 4.45 and 8.19, obtained from Eq. (33) of the preceding section, are considerably larger. The second-order effects of the positron-electron attraction will increase the present enhancement factors, and it is possible that most of the discrepancy can be removed in this way. This point is still under investigation.

Concerning the momentum dependence of the enhancement factors, a detailed study has been carried out and will be published elsewhere.[67] Therefore, only the results will be stated here. We find that the annihilation rate for the fastest electrons is about 10–20% greater than for the slowest. This is contrary to the usual expectation that the slower the electrons are, the more they should be deflected by the Coulomb field. As a matter of fact, the enhancement factor for free electrons is inversely proportioned to their velocity.[68] The electrons in a degenerate gas are not, however, free in the sense that the motion of one electron is independent of the existence of the others. The Pauli exclusion principle plays a predominant role in the present problem, and it is the faster electrons near the surface of the Fermi sea which are more nearly free in the sense of being less restricted by the Pauli principle. This effect is not very pronounced and tends to be masked by the other effects discussed in Sec. A. As the experimental data on metals continue to become more precise, however, it will no doubt eventually be necessary to allow for the momentum dependence of the annihilation rate of the conduction electrons.

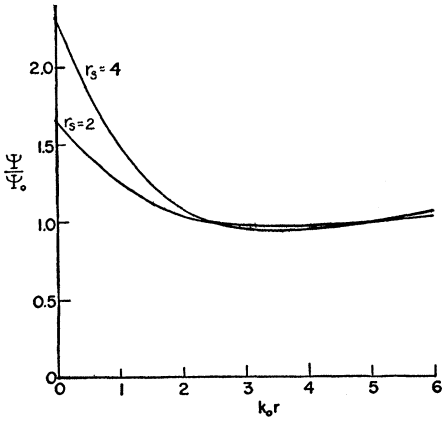

FIG. 15. Positron-electron correlation functions for two different electron densities as a function of the positron-electron separation [in units of (Fermi wave number)$^{-1}$].

An additional complicating effect is illustrated in the lower right hand portion of Fig. 14 and is due to the short range electron-electron interactions. These virtual collisions populate the states outside the Fermi sea with a total probability per electron[69] of

$$\delta=\frac{r_s^2}{29}\left(\frac{0.39}{\beta}-0.35+0.075\beta\right). \tag{54}$$

δ varies from 6.5% for $r_s=2$ to the relatively large value of 14.1% for $r_s=4$. Although annihilation from these high momentum states would contribute to the tails found in the two-photon angular correlation, this contribution is discriminated against by the large enhancement factors for annihilation from the Fermi sea. In addition, the probability of a high momentum component is probably overestimated by Eq. (54). As in the case discussed above of the screening cloud around the positron, the high momentum admixtures due to the electron-electron interactions produce Coulomb holes which are bound closely to the electrons. But for the annihilation it is not these Coulomb holes which matter, but only those in the vicinity of the positron. The latter are probably suppressed by the increased electron density at the positron. We therefore conclude that the contribution of the electron-electron interaction to the two-photon angular correlation tails is probably in most cases negligible compared to that from the excluded volume effect.

D. Relation to X-Ray Emission

The emission of x-rays by a metal is similar to the process of positron annihilation. In both cases an electron drops into a "positive hole," emitting electromagnetic radiation. In the one case the "positive hole" consists of one of the fixed positive ions which lacks an electron in one of its inner shells, while in the other case it is a positron free to move about through the metal. In each case, however, the Coulomb field surrounding the "positive hole" must produce important changes in the electron distribution in its vicinity. As discussed in the preceding two sections, this Coulomb field enhances the positron annihilation rate manyfold. Although it is not feasible to measure the absolute lifetime of the "positive hole" in the case of x-ray emission, it is quite probable that it is also many times shorter than would be the case without the Coulomb attraction. Recently

[67] To be submitted to *The Physical Review*.
[68] See reference 1, p. 134.
[69] D. Pines, reference 48, p. 398.

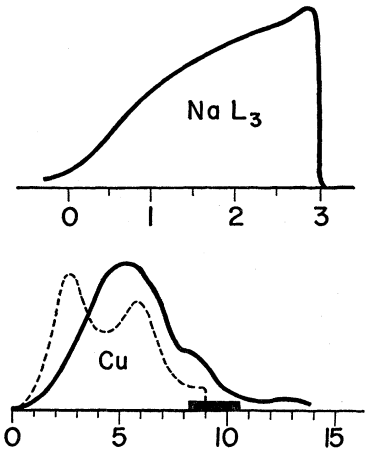

FIG. 16. (After Skinner.) Emitted x-ray intensity for sodium and copper as a function of photon energy (measured in electron volts, above minimum energy).

Friedel[70] has emphasized the importance of screening in interpreting x-ray data. The purpose of this section is to point out some similar Coulomb effects, suggested by the preceding discussion of positron annihilation, in the x-ray emission spectra of a few metals. The theories of positron annihilation and x-ray emission are so similar that it seems desirable that they should proceed hand-in-hand. Advances in one field can be applied in the other, and vice versa.

Although the physical phenomenon in x-ray emission is practically identical to that in positron annihilation, the relative transition rate to the various final states of the system is measured as a function of the energy of the final state rather than its momentum. Thus the two types of experiments complement one another by studying different facets of essentially the same phenomenon. This is an additional reason for adopting a unified viewpoint toward these two fields, and it is to be hoped that a great deal can be learned about various individual metals by correlating x-ray emission and positron annihilation results on the same metal. A particular case in point is sodium, whose emission spectrum is shown in the upper half of Fig. 16.[71] The sharp emission edge at the right, representing the maximum x-ray energy, corresponds to leaving the final system of no "positive hole" and one less conduction electron in its ground state. The rest of the spectrum corresponds to leaving the system in an excited state, and would be expected on the Sommerfeld theory to have a parabolic form with a low-energy cutoff at an x-ray energy shifted to the left of the emission edge by the Fermi energy. The corresponding final state is that of a hole in the one-electron plane wave state of zero energy. There exist, of course, even higher excited stationary states of the system, which consist of at least two holes in (plus one electron outside) the Fermi sea. These, however, cannot be excited by annihilating an electron from the ground state if the latter has no holes to begin with.

The experimental spectrum has qualitatively the expected parabolic shape, but does not exhibit the sharp low-energy cutoff. Instead there is a small tail which extends toward lower energies, and which can be interpreted as due to the presence of holes in the initial state, arising from the electron-electron collisions. The effect of these collisions was estimated by Skinner,[36] and more recently by Landsberg,[72] and is the same as discussed at the end of the preceding section, in connection with the tails in the two-photon angular correlation. The estimate obtained there of $\delta=0.14$ for $r_s=4$ would lead to an excessively large tail, both for the positron annihilation and the x-ray emission. But the reasons given in Sec. C also apply here and result in a tail which is relatively small compared to the main part of the emission band. We have not investigated this question quantitatively, but it seems likely that satisfactory agreement with experiment may be obtained in this way. The Coulomb enhancement alone already reduces the relative size of the tail by a very large factor. Landsberg did not take into account these corrections, and therefore was forced to assume an excessively weak screened Coulomb interaction of the electrons in order to obtain an effect sufficiently weak to agree with experiment.[73]

Another metal in which the attractive effect of the Coulomb field is likely to be important is copper, whose spectrum is also shown in Fig. 16. Here the s electrons will be pulled in to screen out the positive charge, while the d electrons, being in a filled shell, are not as free to correlate. The density of s electrons may therefore be greatly increased at the "positive hole," leading to a proportionally larger x-ray intensity from the s band than is generally assumed. This effect may help to explain the discrepancy between the predicted theoretical curve (dashed line) and the experimental curve (solid line).

According to the preceding section a small fraction of the annihilations should leave the system in an excited state of plasma oscillation. The analysis given there applies also to x-ray emission, which is actually a much better method of detecting the effect, since the final states of the system are separated out according to their energy. The $L_{II,III}$ emission spectrum of magnesium seems to exhibit this effect and actually contains a weak broad line shifted toward longer wavelengths by the Mg plasmon energy of 11 ev, measured from the emission edge. Skinner[74] also mentions such a line for the Al $L_{II,III}$ spectrum, where the shift is 30 ev, or twice the plasmon energy. The creation of two plasmons upon annihilating the "positive hole" is possible but

[70] J. Friedel, Phil. Mag. **43**, 153, 1115 (1952).
[71] The curves in Fig. 16 were prepared from those appearing in the review article of H. W. B. Skinner, Repts. Progr. Phys. **5**, 257 (1938).
[72] P. T. Landsberg, Proc. Phys. Soc. (London) **A62**, 806 (1949).
[73] D. Pines, reference 48, p. 413, discusses the difficulty in reconciling Landsberg's screening length with the value obtained from the Bohm-Pines theory.
[74] H. W. B. Skinner, reference 36, p. 121 and Fig. 9.

would be expected to be less probable than single plasmon creation. The absence of an emission line corresponding to the latter is puzzling. The line might conceivably be masked by the tail from the main emission band. The absence of such a line in the Na $L_{II,III}$ spectrum is probably due to an extreme case of screening, as is possible in such a case of low electron density. The work of Friedel[70] indicates that there is probably some sort of bound state around the "positive hole." The bound electron would screen out the long range interaction of the "positive hole" with the plasma oscillators, resulting in no polarization of the plasma and consequently no virtual plasmons in the initial state.

Plasmon creation upon absorption of x-rays should also occur in all metals which exhibit plasmon creation upon emission. This is because the state obtained as a result of the x-ray absorption must be expanded in terms of the stationary states of the coupled system of the "positive hole" and the conduction electrons. If there is polarization of the plasma there will be nonzero probability amplitudes in the expansion corresponding to the stationary states of plasma oscillation. Thus the absorption edge should appear reproduced and shifted toward shorter wavelengths by the plasmon energy, and show up in the so-called fine structure of the x-ray absorption. The general appearance of such fine structure, correlated in a wide variety of metals with the characteristic energy losses, was noted by Leder *et al.*[75] By making the tacit assumption that the fine structure was exclusively of the Kronig type, or at least arose from interaction with the lattice, these authors inferred that the corresponding characteristic energy losses must all be of a nonplasma nature. From the above discussion it is clear that this assumption is by no means required and that the Bohm-Pines plasma theory offers a quite natural interpretation of the correlation noticed by Leder *et al.*

IV. POSITRONIUM IN INSULATORS

A. Lifetime

It is generally accepted that the long lifetime, or "τ_2 component," discovered by Bell and Graham[3] in many insulators, is due to the formation of orthopositronium. Orthopositronium, when isolated from other atoms and perturbing fields decays by three-photon emission. Consequently the two-photon counting rate must be reduced in those solids exhibiting the τ_2 component. This has been observed by Pond.[76] The three-photon rate itself has been measured by DeBenedetti and Siegel,[77] Graham and Stewart,[78] and Wagner and Hereford.[79] A typical case investigated by Bell and Graham is shown in Fig. 17 where the logarithm of the

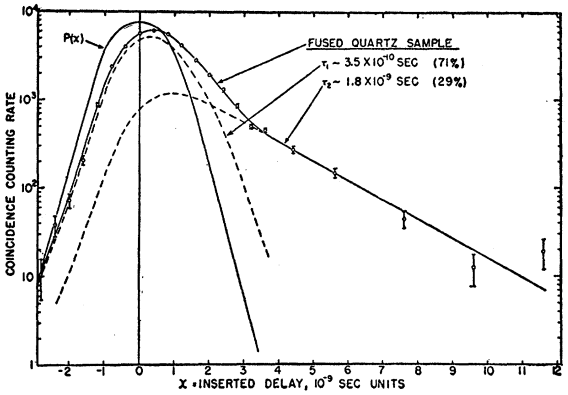

FIG. 17. (After Bell and Graham.) Annihilation photon counting rate for fused quartz as a function of time delay (in 10^{-9} sec).

annihilation rate of positrons in fused quartz is plotted against time delay. They find, by extrapolating the linear portion of the curve to the left, that the τ_2 component contains 29% of the counts, with a decay constant of $\tau_2 = 1.8\times10^{9}$ sec. This is typical of the τ_2 values found by Bell and Graham, which are all of the order of 10^{-9} sec. The $2s$ state of parapositronium happens to have a lifetime eight times that of the $1s$ state, or precisely 10^{-9} sec. This coincidence has led Dixon and Trainor[80] to suggest that this excited state of positronium is responsible for the τ_2 component. Longer values of τ_2, up to 4×10^{-9} sec, can be obtained by assuming rapid *para-ortho* conversion. Wallace[4] has pointed out that the hypothesis of Dixon and Trainor is untenable because of the rapid de-excitation of positronium which can be expected in solids. An additional difficulty, although not so conclusive, is that the Ore gap is always much smaller for the excited states than for the ground state. The ground-state binding energy of ry/2 must be replaced in Inequality (1) by ry/8, in dealing with the energetics of $2s$ formation. Even if the inequality is satisfied for the $1s$ state it may very well not be satisfied for the $2s$ state. Therefore we must regard capture into the ground state as the dominant mode of positronium formation. The few positronium atoms which are formed in excited states will quickly break up, if there is no Ore gap for these states, or be quickly deexcited to the ground state. In interpreting the τ_2 component it seems that one should take only the ground state into consideration.

Ortho-para conversion has been suggested by Bell and Graham to account for their values of τ_2. There is, however, no reason to expect such a conversion in the insulators exhibiting the τ_2 component. These all consist of atoms with closed shells, in which the electron spins are paired off. There can therefore be no conversion by electron exchange. (The situation is, of of course, quite different in metals, as discussed in Section IIIB above.) If the weak effect of electrostatic

[75] Leder, Mendlowitz, and Marton, Phys. Rev. **101**, 1460 (1956).
[76] T. A. Pond, Phys. Rev. **93**, 478 (1954).
[77] S. DeBenedetti and R. T. Siegel, Phys. Rev. **94**, 955 (1954).
[78] R. L. Graham and A. T. Stewart, Can. J. Phys. **32**, 678 (1954).
[79] R. T. Wagner and F. L. Hereford, Phys. Rev. **99**, 593 (1955).
[80] W. R. Dixon and L. E. H. Trainor, Phys. Rev. **97**, 733 (1955).

fields is neglected (see IVC later), one finds the orthopositronium atoms remain as such and have a zero two-photon annihilation rate. The slow three-photon rate would lead to a lifetime of $\sim 10^{-7}$ sec, and can be neglected here. Thus, the positron in orthopositronium is stable with respect to annihilation with its own electron, and can only decay by "pickoff" annihilation with an electron belonging to one of the surrounding atoms in the solid.[81]

Of all the condensed materials exhibiting the τ_2 component, liquid helium seems the simplest to deal with theoretically. Most of our discussion of this case can be applied to the general case of the insulating solids. Graham *et al.*[82] report $\tau_2=(2.7\pm 0.3)\times 10^{-9}$ sec. A rough theoretical estimate is obtained from the average density of electrons, which is most easily specified by the radius, $r_s' a_0$, of the unit atomic sphere. The present parameter is primed to distinguish it from the somewhat similar parameter used in the theory of metals. The density of liquid helium at the boiling point[83] is 0.127 gm/cm^3, from which one can calculate the atomic volume. Equating the latter to $4\pi r_s'^3 a_0^3/3$ one obtains $r_s'=4.35$. The ratio of the electron density to that in positronium is consequently

$$2(4\pi r_s'^3 a_0^3/3)^{-1}/(8\pi a_0^3)^{-1}=12/r_s'^3=1/6.85,$$

corresponding to a lifetime of 3.42×10^{-9} sec. This value is of the right order of magnitude but slightly longer than the experimental value of τ_2. Most of the prompt τ_1 decay is presumably due to positrons which have "missed the Ore gap" and are stopped without forming positronium. These positrons are attracted to the helium atoms by a polarization force and their wave function is concentrated at the surface of the atoms, similar to the situation around the negative ions in the ionic crystals. Thus the nonpositronium positrons are predominantly in regions of high electron density, which explains their rapid annihilation rate. It should be emphasized that the prompt mode of decay is actually complex and composed of two parts. There is a small percentage (one-third of the τ_2 percentage) of parapositronium decay with the very short lifetime of 1.25×10^{-10} sec. The bulk of the τ_1 component is however made up of the nonpositronium decay referred to above, and with generally somewhat longer lifetime.

There is also a weaker polarization force, of the Van der Waals type, between a positronium and a helium atom. It will considerably reduce the theoretical lifetime of the orthopositronium atoms. Actually, there are two different types of forces acting on the positronium atoms, which tend to compensate one another. Besides the attractive Van der Waals force there is the repulsive exchange force. The positronium atom is excluded from the interior of a filled shell atom, since the exclusion principle does not allow the positronium electron to be in a region already "saturated" by electrons. The exchange force works in general against the pickoff annihilation and is probably the dominant reason in most materials for the long lifetime. The Van der Waals force seems to compensate for this effect in liquid helium, where we have seen that the pickoff rate is already slow enough to account for the τ_2 component, without the exchange force. Nevertheless, we make here a rough calculation of the exchange force for helium, which may serve as a prototype for cases where the effect of exchange predominates. We shall also use the result of the calculation in discussing the Ore diagram for liquid helium.

Let the helium nucleus be at the origin, and the coordinates of the spin up positron, the spin up positronium electron, and the spin up helium electron be $\mathbf{x}_0$, $\mathbf{x}_1$, and $\mathbf{x}_2$, respectively. The spin down helium electron does not exchange and will be ignored here. Let the positronium atom be relatively far away from the helium atom, and with wave function $\psi(\mathbf{x})\chi(\mathbf{X})$, where $\mathbf{x}=\mathbf{x}_1-\mathbf{x}_0$ and $\mathbf{X}=(\mathbf{x}_1+\mathbf{x}_0)/2$. ψ and χ are the internal and center-of-mass wave functions of the positronium atom. The total potential energy consists of, aside from the part belonging to the helium and positronium atoms separately, (1) an interaction of the helium and positronium electrons, (2) an attraction between the helium electron and the positron, and (3) an interaction between the helium nucleus and the positronium atom. (1) is a minor effect in this type of problem and will be neglected. It would of course have to be included in a more exact treatment. An additional simplifying feature of the present problem is that (2) may be neglected. This is due to the tight binding of helium compared to the relatively loose positronium binding. The overlap of the electron wave functions is close to the helium nucleus and far from the positron. Therefore we concentrate on (3) and calculate its expectation value. The direct integral vanishes because of the symmetry of $\psi=e^{-|\mathbf{x}_1-\mathbf{x}_0|/2a_0}/(8\pi a_0^3)^{\frac{1}{2}}$ with respect to interchange of the positron and electron.[84] This leaves only the exchange integral

$$E_{\text{ex}}=-\int\int\int d^3\mathbf{x}_0 d^3\mathbf{x}_1 d^3\mathbf{x}_2 \phi^*(\mathbf{x}_1)\psi^*(\mathbf{x}_2-\mathbf{x}_0)\times\chi^*\left(\frac{\mathbf{x}_2+\mathbf{x}_0}{2}\right)\cdot\frac{-2e^2}{x_1}\cdot\phi(\mathbf{x}_2)\psi(\mathbf{x}_1-\mathbf{x}_0)\times\chi\left(\frac{\mathbf{x}_1+\mathbf{x}_0}{2}\right). \quad (55)$$

ϕ is the wave function of the helium electron and

[81] The possibility of this process has been mentioned by R. L. Garwin, Phys. Rev. **91**, 157(L) (1953) and M. Dresden, Phys. Rev. **93**, 1413(L) (1954).

[82] Graham, Paul, and Henshaw, Bull. Am. Phys. Soc. Ser. II, **1**, 68 (1956).

[83] C. F. Squire, *Low Temperature Physics* (McGraw-Hill Book Company, Inc., New York, 1953), p. 66.

[84] In this respect the present problem is simpler than the well-known analogous problem of the He—H short-range repulsion.

vanishes except for values of the argument near the origin. Therefore the remaining factors, for large $|\mathbf{x}_0|=x_0$ can be approximated by setting $\mathbf{x}_1=\mathbf{x}_2=0$. In this approximation we also have $\mathbf{x}_0=2\mathbf{X}$ so that Eq. (55) becomes

$$E_{ex}=\int d^3\mathbf{X}|\chi(\mathbf{X})|^2U(\mathbf{X}), \tag{56}$$

where

$$U(\mathbf{X})=\text{ry}\ e^{-2X/a_0}\cdot\frac{4}{\pi a_0^2}\int d^3\mathbf{x}_1\frac{\phi(\mathbf{x}_1)}{x_1}\int d^3\mathbf{x}_2\phi(\mathbf{x}_2). \tag{57}$$

By inserting the approximate expression[85] $\phi(\mathbf{x})=e^{-x/a}/(\pi a^3)^{\frac{1}{2}}$, where $a=a_0/Z'$ and Z' is the effective screened nuclear charge of $27/16=1.687$, it is a simple matter to reduce Eq. (57) to

$$U(\mathbf{X})=(128/Z'^2)\ \text{ry}\ e^{-2X/a_0}. \tag{58}$$

A somewhat more convenient form of this equation is

$$U(\mathbf{X})=0.824\ \text{ry}\ e^{-2(X-2a_0)/a_0}, \tag{59}$$

which emphasizes the fact that the approximations on which Eq. (57) is based fail completely for separations less than one angstrom. The exchange energy is negligible for separations from $3a_0$ out to $4.35a_0$, the radius of the unit atomic sphere. It increases rapidly in the neighborhood of $X=2a_0$ and tends to prevent separations of less than an angstrom. Such a short-range repulsion, which must always be present, not only for neutral atoms, but for ions consisting of filled electron shells, guarantees a moderate pickoff annihilation rate.

From the above paragraph it is clear that if positronium is formed at all in an insulator the atoms in the triplet state will exhibit the long τ_2 lifetime. Only the question of the existence of the Ore gap remains. This has been discussed in Sec. IIA above, where it is shown that the determining factors are the (1) electron, (2) positron, and (3) positronium affinities. These can be estimated roughly for liquid helium. Beginning with (3), let us replace the exchange repulsion with a rigid sphere at a radius of $2a_0$. Then the positronium atoms have a "free run" from one helium atom to the next of $2(r_s'-2)a_0=4.70a_0$, corresponding to a negative positronium affinity of 0.223 ry=3.03 ev. Both (1) and (2) are also negative and probably fairly large. We need here only the sum, which can be estimated very roughly by using plane waves for both the electron and positron. In calculating the expectation value of the total Coulomb energy the direct integrals cancel. The exchange integral for the electron-nucleus interaction is, if we use the same notation as above,

$$E_{ex}'=-\frac{3}{4\pi r_s'^3a_0^3}\int\int d^3\mathbf{x}_1d^3\mathbf{x}_2\phi^*(\mathbf{x}_1)\frac{-2e^2}{x_1}\phi(\mathbf{x}_2)$$

$$=(96/r_s'^3Z'^3)\ \text{ry}=0.409\ \text{ry}=5.55\ \text{ev}. \tag{60}$$

[85] See reference 20, p. 176.

The constant in front of the integral comes from the normalization of the electron wave function. Thus, the sum of the electron and positron affinities in liquid helium is even more negative than the positronium affinity. This would lead one to expect a higher percentage of positronium formation in liquid than in gaseous helium. This seems to be the case experimentally.[82] Although the exact values of the affinities will be affected by the adjustment of the wave functions to the field of the helium atom, as well as by polarization effects, it is clear that Inequality (1) is easily satisfied in the case of liquid helium.

The question of the existence of the Ore gap is difficult to answer in general. The answer can be found, in any given case, from the affinities. As discussed in detail in Sec. IIA, the most important factor is generally the positronium affinity. For positronium formation there must always be room in the material for the positronium atom. This seems to be the case in liquid helium, and is probably also the case in such amorphous substances as fused quartz, Teflon, etc. The ionic crystals are unfavorable in this respect because they are so closely packed. The crystalline structure itself is, however, not particularly unfavorable to positronium formation, provided it is sufficiently open with enough space between the atoms. An example is ice, which exhibits[3] (at 77°K) a slow component with $\tau_2=(1.2\pm0.2)\times10^{-9}$ sec. On the other hand, a noncrystalline structure does not, by any means, guarantee an Ore gap. Examples are liquid argon and liquid nitrogen, which do not exhibit a τ_2 component. The atoms in these liquids are heavier than in helium and have less zero point motion. The liquids are consequently more densely packed and evidently do not provide enough room for positronium. Thus, the regularity or irregularity in the arrangement of the atoms of a substance seems to be largely irrelevant to positronium formation. The determining factor seems to be the gross density, at least in the case of a liquid or crystal. In the amorphous solids cavities and defects may locally provide room for positronium atoms even in cases where the gross density itself may not be favorable.

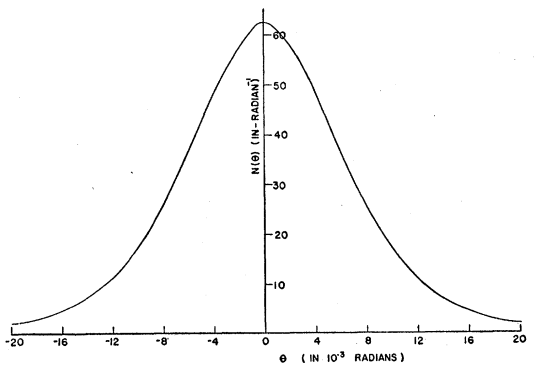

FIG. 18. Two photon angular correlation for pickoff annihilation of orthopositronium positrons in helium.

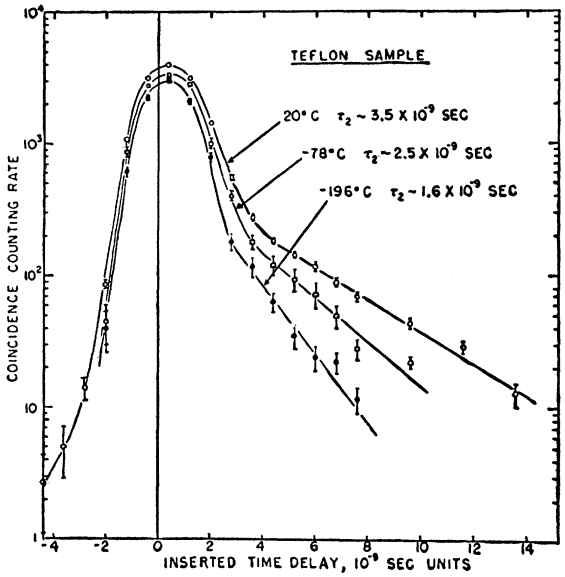

FIG. 19. (After Bell and Graham.) The temperature dependence of the long lifetime in Teflon.

The two-photon angular correlation for the pick-off mode of decay is easily estimated. Because of the looseness of the positronium binding, the positron momentum can be neglected compared to that of the tightly bound atomic electron with which it annihilates. Thus, the two-photon angular correlation should measure roughly the momentum distribution of the atomic electron. A typical case is shown in Fig. 18, where the number of counts to be expected from the τ_2 component in liquid helium is plotted against angle. The essential general feature of the pickoff mode of decay is that it gives a broad distribution, similar to that from the nonpositronium part of the τ_2 component. Such broad distributions have been bound experimentally for fused quartz by Page *et al.*[86] and for Teflon by Stewart.[38] Superposed on their broad distributions are narrow distributions of an intensity, as they point out, somewhat greater than can be accounted for by the decay of parapositronium alone. The origin of this additional narrow distribution is discussed in Sec. C below. The point to emphasize here is that most of the τ_2 component appears in the broad distribution, as should be the case for pickoff annihilation.

B. Temperature Effect

In their investigation of the long lifetimes Bell and Graham discovered a marked temperature dependence of τ_2 for all solids investigated, except fused quartz. (It may be that this substance would also show the effect if raised to temperatures comparable to its melting point.) The lifetime generally increases with temperature. A typical example is Teflon, where τ_2 doubles as the temperature is raised from that of liquid air to room temperature. The results of Bell and Graham are reproduced in Fig. 19. A particularly convenient way of studying the temperature effect experimentally is to measure the three-photon counting rate, which is proportional to the population of orthopositronium. This population is simply equal to the rate of orthopositronium production times τ_2. As long as no significant change takes place in the solid upon heating, one may assume that the production rate is temperature independent. This has been verified by Bell and Graham[3] for ice, Teflon, and polystyrene, and it is probably safe to assume that it holds provided no phase transition occurs. When the latter happens, the energetics of the Ore gap may change, thereby affecting the rate of positronium formation. Wagner and Hereford have measured the three-photon rate for a number of solids, and their results for methyl alcohol, ice, and glycerine are reproduced in Fig. 20. The ordinate can be taken, according to the above discussion, as proportional to τ_2. The temperature effect is particularly striking in glycerine, where the variation is by more than a factor of two.

The temperature dependence of τ_2 is perhaps the most puzzling and least understood effect in the entire subject of positron annihilation in solids. So far, the most satisfactory explanation seems to be that of Wallace,[4] who suggests that the positronium atoms adiabatically respond to the motions of the atoms or molecules of the solid. Because of the repulsive exchange force discussed above, for any instantaneous configuration of the solid the positronium atoms tend to concentrate into regions as far away from the atoms of the solid as possible. In other words, the positronium atoms seek out "holes," and thereby not only lower their energy but their pickoff annihilation rate. The temperature effect results from the thermal agitation, which produces such density fluctuations, or "holes." An individual positronium atom, for example, may happen to be situated in a "hole" formed between two atoms which happen to be displaced in opposite directions. As the atoms move back together the positronium atom will leave the region between the atoms and pass on to some other location where there now happens to be a

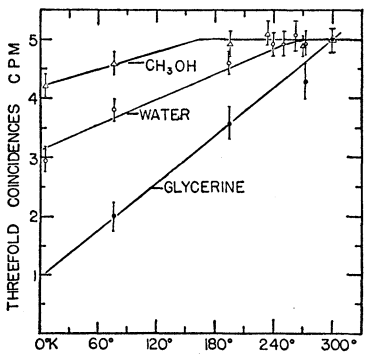

FIG. 20. (After Wagner and Hereford.) The temperature dependence of the three-photon counting rate in methyl alcohol, water, and glycerine.

[86] Page, Heinberg, Wallace, and Trout, Phys. Rev. 98, 206 (1955).

new "hole" present. A similar, but more idealized and simpler situation is the trapping of the positronium atom by an individual sound wave. The positronium atom rides along in the trough of the wave and always experiences a lower atomic density than is the average for the crystal. At absolute zero there is no effect since the sound wave is not excited. Near the melting point, if we concentrate all the thermal excitation into the one sound wave we might expect a maximum decrease in atomic density in the vicinity of the positronium atom of about 10%. This density change is about the same as takes place in the bulk density of liquid He upon passing from the λ point to the boiling point. According to Graham *et al.*[82] a 30% increase results in the value of τ_2. Thus, a general temperature effect of this order of magnitude would be expected, but it is difficult to understand the observed very large increases in τ_2.

C. Narrow Component

A narrow component in the two-photon angular correlation is strong evidence of positronium. It can only result from decay of a positronium positron with its own bound electron.[87] Other modes of decay, such as pickoff annihilation of positronium or annihilation of nonpositronium positrons,[87] give a broad distribution. Furthermore, a narrow component is evidence that the positronium atoms have been slowed down to relatively low energies. For example, a half-breadth of $\theta=P/mc=2$ milliradians, where P is the positronium momentum, corresponds to an energy of

$$P^2/4m=(mc^2/4)(P/mc)^2=10^{-6}mc^2=0.5 \text{ ev}.$$

This is twenty times the thermal energy of 0.025 ev (at room temperature), but is nevertheless small compared to the average energy the positronium atoms possess upon formation. That thermalization should not be complete is in agreement with Wallace's[4] estimate.

As mentioned in Sec. A, the narrow component found by Page *et al.*[86] in the two-photon angular correlation for fused quartz has an intensity somewhat greater than can be accounted for solely on the basis of parapositronium decay. According to Bell and Graham[3] the percentage of orthopositronium formation in fused quartz is 29%. The parapositronium percentage must amount to one-third of this, or about 10%. Figure 21, which has been prepared from the paper of Page *et al.*, shows the distribution for fused quartz (dashed curve labeled "F") superposed on the broad distribution for crystalline quartz (solid curve labeled "C"). They estimate the area between the two curves at 18% of the total area under the fused quartz curve. Thus, there is an additional 8% which must be atrributed to *ortho-para* conversion. Since there are no unpaired electrons to exchange, the conversion must be due to spin flip by magnetic fields. Although there was no static magnetic field present in this experiment, the motion of a positronium atom across the electrostatic lines of force produces a magnetic field in the positronium Lorentz frame of

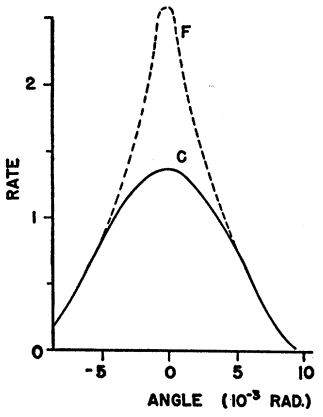

FIG. 21. (After Page, Heinberg, Wallace, and Trout.) The two-photon angular correlation for crystalline (C) and fused (F) quartz.

$$\mathfrak{H}=-(\mathbf{V}/c)\times\mathcal{E}=-(\tfrac{1}{2}mc)\mathbf{P}\times\mathcal{E}, \qquad (61)$$

where $\mathcal{E}$ is the electric field vector and $\mathbf{V}$ and $\mathbf{P}$ the positronium velocity and momentum, respectively. The magnitude of $\mathfrak{H}$ can be estimated from $(29\%/8\%)\times1.8\times10^{-9}$ sec, the effective *ortho*-lifetime without competing pickoff annihilation. The free space *ortho*-lifetime is longer than this by the factor 1.38×10^{-7} sec$/6.5\times10^{-9}$ sec$=21$, which is in general given by the formula[88] $1+(\mathfrak{H}/2190 \text{ gauss})^2$. Hence we find $\mathfrak{H}=9800$ gauss. But $P/mc=\theta$, and the average value of θ for the narrow component of Fig. 21 is about 2 milliradians. Thus, from Eq. (61) we obtain

$$\mathcal{E}\approx(2/\theta)\mathfrak{H}\approx10^7 \text{ esu}\approx30 \text{ volt/A}$$
$$\approx2.5 \text{ ry}/e\text{A}\approx2.5\ e/\text{A}^2. \qquad (62)$$

This is, of course, an extremely strong electric field, but is of about the order of magnitude to be expected in the interstitial regions of fused quartz, between the Si^{4+} and the O^{2-} ions. Actually, as discussed in Sec. A above, the positronium is probably localized at holes and defects, where the electric field is considerably weaker. Furthermore, positronium cannot exist as a bound system in the presence of such a strong field as that given by Eq. (62).[89] Even a field an order of magnitude weaker would ionize the atoms at a fairly rapid rate. Thus, although the mechanism proposed here is qualitatively satisfactory, it seems to be much too ineffective. The intensity of the narrow component cannot be considered as understood at the present time. A difficult but crucial experiment would be the determination of the two-photon angular correlations separately for the τ_2 and the τ_1 components. Using a

[87] Here we seem to differ from Wallace, reference 4, who would attribute the narrow component to the decay of positrons bound to the atoms or molecules of the solid.

[88] T. A. Pond and R. H. Dicke, Phys. Rev. **85**, 489 (1952).

[89] The author has benefited from a discussion with Professor M. Deutsch on this point.

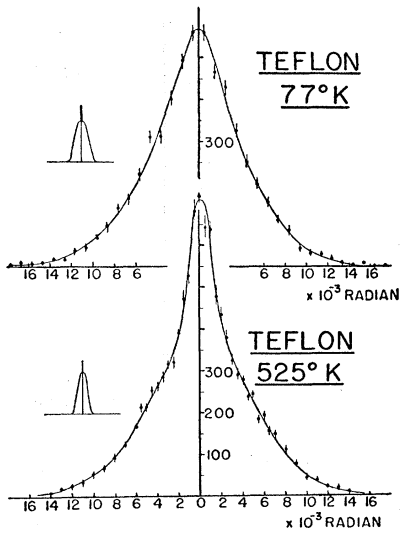

FIG. 22. (After Stewart.) The temperature dependence of the narrow component in Teflon.

Na^{22} source, one could measure the correlation for the prompt τ_1 component by requiring triple coincidence among the Na^{22} gamma ray and the two annihilation quanta. Suitably normalizing the resulting curve and subtracting it from the fused quartz curve obtained by Page's group should reveal directly the fraction of the τ_2 component which undergoes *ortho-para* conversion.

If one accepts some *ortho-para* conversion whose rate is relatively temperature independent, one can understand the high-temperature enhancement of the narrow component found in Teflon by Stewart. Stewart's[38] measurements at 77°K and 525°K are reproduced in Fig. 22. There seems to be a much stronger narrow component at the higher temperature. This can be understood on the basis of the temperature dependence of τ_2. As the temperature is raised τ_2 increases, which must be due to a decrease in the pickoff annihilation rate. The *ortho-para* conversion can then compete more favorably, and a larger fraction of the τ_2 component shows up in the narrow portion of the two-photon angular correlation.

Additional *ortho-para* conversion can be "artificially" induced by applying a strong external static magnetic field, of the order of 10 000 gauss. The resulting enhancement of the narrow component has been observed by Page *et al.*,[90] while Telegdi[26] has measured the associated decrease in the three-photon rate. These experiments lend support to the general picture of positronium in solids.

V. SUMMARY

The status of the theory of positron annihilation in solids is on the whole encouraging. There is enough agreement between theory and experiment to warrant considerably more theoretical work. Especially in need of further attention are the case of an electron gas of low density, where there is likely to be positronium of a sort present, and the case of positronium in insulators, where the mysterious temperature effect and narrow component still need explanations. Extension of the experimental measurements to the alkali metals of lower electron density might help to guide the theory in the first case. In the insulators, measurement of the two-photon angular correlation of the τ_2 and τ_1 components separately would be of great importance.

In the case of the ionic crystals, further theoretical work on the wave function of the positron should lead to a value for the lifetime. It should be also possible to estimate the extent of polarization. Further experimental measurements of the lifetimes for various alkali halides would provide a test of the calculations.

Another type of experiment suggested by the theoretical discussion of the preceding sections is the measurement of the two-photon angular correlation for oriented crystals. The excluded volume effect, being associated with the periodic lattice, should show a dependence on orientation. Thus copper should be a particularly promising case to investigate. Crystals of the alkali halides may also show some anisotropy, since the field around the halide ions, which determines the positron wave function, has by no means complete spherical symmetric.

APPENDIX. THE ANNIHILATION PROCESS

In this appendix we evaluate the universal constant of proportionality by which expression (iii) of the introduction should be multiplied. The absolute annihilation rate can then be calculated for any electron-positron system for which the initial wave function is known. Since we are only interested in slow electrons and positrons we can achieve a great simplification over the usual calculation[91,92] of annihilation in flight, which uses trace techniques so as to avoid introducing explicitly the electron and positron spinor wave functions. Here the matrix element for the annihilation process can be calculated for an electron and positron at rest. For this special case the spinor wave functions are especially simple, and the calculation is most conveniently carried out by introducing them directly. The adjoint of the Dirac spinor for an electron at rest,

[90] Page, Heinberg, Wallace, and Trout, Phys. Rev. **99**, 665 (1955).

Note added in proof.—See also L. A. Page and M. Heinberg, Phys. Rev. **102**, 1545 (1956). At the International Conference on Quantum Interactions of the Free Electron, University of Maryland, April, 1956, M. Deutsch reported that the τ_2 component is split by an external magnetic field into a complex decay consisting of two parts—a situation already familiar from the experiments in gases. The larger part decays with the zero field value of τ_2 and is attributed to the $m=\pm 1$ triplet states. The $m=0$ state corresponds to the smaller part and has its decay rate enhanced by the magnetic field.

[91] P. A. M. Dirac, Proc. Cambridge Phil. Soc. **26**, 361 (1930).

[92] W. Heitler, *The Quantum Theory of Radiation* (Oxford University Press, London, 1936).

with spin in the x_3-direction, is $(1, 0, 0, 0)$. The electron with its spin flipped and recoiling along the negative x_3 axis is easily shown to be represented[93] by

$$(0, [2\sqrt{2}(\sqrt{2}-1)]^{-\frac{1}{2}}, 0, [(\sqrt{2}-1)/2\sqrt{2}]^{\frac{1}{2}})$$

A positron at rest, with spin in the negative x_3 direction, is treated as a hole in the negative energy state represented by $(0, 0, 1, 0)$. These are the only spinors which we need for the calculation. Let us calculate the second order Hamiltonian matrix element for the creation, by an electron-positron pair in the singlet state, of two photons propagating in opposite directions and each circularly polarized along its direction of propagation, i.e. right circularly polarized. Taking the x_3 axis along one of the propagation vectors one can write the spin function of the electron-positron pair as $(1/\sqrt{2})\times(\alpha_1\beta_2-\beta_1\alpha_2)$ where 1 and 2 denote the electron and positron respectively. Since, from general principles,[2] the triplet state does not emit two photons, it will be sufficient to calculate the matrix element for the initial wave function $\alpha_1\beta_2$, representing a spin up electron and a spin down positron, and multiply the result by $\sqrt{2}$. The perturbation which couples the matter to the radiation field is $H'=e\boldsymbol{\alpha}\cdot\mathbf{A}$, where the components of $\boldsymbol{\alpha}=(\alpha_1, \alpha_2, \alpha_3)$ are the Dirac 4×4 matrices and

$$\mathbf{A}=c\left(\frac{2\pi\hbar}{V}\right)^{\frac{1}{2}}\sum_{\mathbf{k}r}\frac{\boldsymbol{\varepsilon}_{\mathbf{k}r\mu}}{(\omega_{\mathbf{k}})^{\frac{1}{2}}}a_{\mathbf{k}r\mu}{}^{*}e^{-i\mathbf{k}\mathbf{x}}$$

is the photon-creating part of the vector potential. The $\boldsymbol{\varepsilon}_{\mathbf{k}r\mu}$ are unit polarization vectors transverse to the propagation vector $\mathbf{k}$, V is the volume of quantization, and the other symbols have their usual meaning. If we define

$$\alpha_{\mathbf{k}\pm}=2^{-1}(\boldsymbol{\varepsilon}_{\mathbf{k}1}\pm i\boldsymbol{\varepsilon}_{\mathbf{k}2})\cdot\boldsymbol{\alpha}$$

then the part of H' which creates right circularly polarized photons is

$$H'_{+}=2^{\frac{1}{2}}ec\left(\frac{2\pi\hbar}{V\omega}\right)^{\frac{1}{2}}\sum_{\mathbf{k}}\alpha_{\mathbf{k}-}a_{\mathbf{k}+}{}^{*}e^{-i\mathbf{k}\mathbf{x}}$$

where

$$a_{\mathbf{k}+}{}^{*}=2^{-\frac{1}{2}}(a_{\mathbf{k}1}{}^{*}+ia_{\mathbf{k}2}{}^{*}).$$

The energy denominator for the second-order process is $-\sqrt{2}mc^2$ while the numerator contains, besides the factor $[2^{\frac{1}{2}}ec(2\pi\hbar/V\omega)^{\frac{1}{2}}]^2$, the product of the matrix elements of $\alpha_{\mathbf{k}}$ between the initial and intermediate states and between the intermediate and final states. The spinors representing these states have been exhibited above, and it is easily shown that the product of the two matrix elements is simply $(2\sqrt{2})^{-1}$, the product of the spinor components of the intermediate state. This quantity is canceled by the factor of $\sqrt{2}$ which makes our second-order matrix element correct for a pure singlet initial state, and by a factor of 2, which allows for the fact that the intermediate state in which the positron recoils yields an identical contribution. The second-order matrix element for the singlet annihilation is therefore

$$H_s{}^{(2)}=-2^{\frac{3}{2}}\pi e^2\hbar^2/Vm^2c^2. \tag{63}$$

According to time department perturbation theory, the rate of annihilation, averaged over spin orientations, is

$$\frac{2\pi}{\hbar}\rho(E)\,|H^{(2)}|^2V \tag{64}$$

times the expectation value of expression (iii) of the Introduction. $|H^{(2)}|^2$ is one-fourth the square of $H_s{}^{(2)}$ while the factor of V arises upon passing from (ii) to (iii). The density of the two-photon states with respect to energy is

$$\rho(E)=\frac{4\pi k^2dk}{d(2\hbar ck)}\cdot\frac{V}{8\pi^3}=\frac{Vm^2c}{4\pi^2\hbar^3}. \tag{65}$$

Here we have integrated the directions of the photons only over 2π steradians, but have obtained an additional factor of 2 from the left circularly polarized photon states, which have the same second-order matrix element. Substituting Eqs. (63) and (65) into (64) gives $\pi r_0{}^2c$ where $r_0=e^2/mc^2$ is the classical radius of the electron. The annihilation rate is therefore $\pi r_0{}^2c$ times the expectation value of (iii). The latter is $\frac{1}{8}\pi a_0{}^3$ for the positronium atom, which is a convenient reference case. The positronium spin-averaged annihilation rate is consequently

$$r_0{}^2c/8a_0{}^3=(\alpha^4/8)(c/a_0)=2.01\times10^9\ \text{sec}^{-1}, \tag{66}$$

where $\alpha=1/137$ is the fine structure constant.

[93] See reference 20, p. 327.